Available online at www.sciencedirect.com
ScienceDirect
Journal of Photochemistry and Photobiology C: Photochemistry Reviews
7 (2006) 211–230
Journal of Photochemistry and Photobiology C: Photochemistry Reviews
www.elsevier.com/locate/jphotochemrev

Review

Photochemical kinetics uncertainties in modeling Titan's atmosphere: A review

E. Hébrard [a,*], M. Dobrijevic [b], Y. Bénilan [a], F. Raulin [a]

[a] *Laboratoire Interuniversitaire des Systèmes Atmosphériques (LISA, CNRS, Université Paris XII, Université Paris VII UMR 7583), 94010 Créteil Cedex, France*
[b] *Laboratoire d'Astrodynamique, d'Astrophysique et d'Aéronomie de Bordeaux (L3AB/OASU, CNRS, Université Bordeaux 1 UMR 5804), BP 89, 33270 Floirac, France*

Received 31 October 2006; received in revised form 30 December 2006; accepted 31 December 2006
Available online 26 January 2007

Abstract

This paper is a review dealing with the photochemistry of Titan's atmosphere and its sources of uncertainties. It presents current knowledge on the active photochemistry occurring in Titan's atmosphere. A brief discussion of major dissociation paths and essential chemical reactions is given, which allows us to emphasize on the photochemical processes that are still not well represented in the models and might thus be contributing mostly to the overall imprecision of theoretical results. We present a method to evaluate uncertainty factors of the chemical rate constants at temperatures representative of Titan's atmosphere. This compilation can be used as a reference for future uncertainty propagation analysis in Titan's photochemical models developed in the frame of the Cassini–Huygens mission.

Keywords: Chemical uncertainties; Titan; Photochemistry; Monte-Carlo

Contents

* Corresponding author. Tel.: +33 1 4517 15 50; Fax: +33 1 4517 15 64.
E-mail addresses: hebrard@lisa.univ-paris12.fr (E. Hébrard), Michel.Dobrijevic@obs.u-bordeaux1.fr (M. Dobrijevic), benilan@lisa.univ-paris12.fr (Y. Bénilan), raulin@lisa.univ-paris12.fr (F. Raulin).

1389-5567/$20.00 © 2007 Elsevier B.V. All rights reserved.
doi:10.1016/j.jphotochemrev.2006.12.004

Eric Hébrard was born in Lyon, France. He received his diploma in chemistry in 2002 from the Ecole Normale Supŕieure (Paris, France) after a 1-year internship working on mineral catalysis of RNA prebiotic synthesis in the New York Center for Studies on the Origins of Life, a NASA Specialized Center of Research and Training led by James P. Ferris (Rensselaer Polytechnic Institute, Troy, USA). In 2003, he started his PhD research at the Laboratoire Interuniversitaire des Systémes Atmosphériques (Créteil, France) in the Groupe de Physico-Chimie Organique Spatiale (GPCOS) led by Franois Raulin. His research involved some theoretical aspects of the photochemical processes occuring in Titan's atmosphere, and more specifically the way uncertainties in the photochemical kinetic data could affect computed simulations and their subsequent comparisons with observations. He obtained his PhD in 2006 and is now a postdoctoral fellow at the Centre National d'Etudes Spatiales (CNES) simulating aeolian erosion thresholds on Mars in order to improve the predictions of atmospheric dust activity and its possible impacts on Martian chemistries.

Michel Dobrijevic is an assistant professor at the University of Bordeaux, Talence, France and a member of the Laboratoire d'Astrophysique, d'Astrodynamique et d'Aéronomie de Bordeaux, Floirac, France. He was born in Paris, France. He obtained his diploma in theoretical physics from the University of Bordeaux, France in 1992 and the PhD in 1996 on the modeling of photochemical processes in the atmosphere of the giant planet Neptune (University of Bordeaux, France). His main research activities concern the study of planetary atmosphere and astrobiology. His present research interests concern the modeling of physical and chemical processes that govern the complexification of organic matter in the atmosphere of Titan. He is also a principal investigator for a project of a spatial micro-array dedicated to the search of organics in planetary surfaces.

Yves Benilan is a research scientist of the French National Research Council (CNRS). He joined the "Laboratoire Interuniversitaire des Systme Atmosphériques" (LISA, Université Paris 12) in 1993 on the occasion of his PhD thesis on the mid-UV spectroscopy of organic compound and its application to the study of Titan's atmosphere (University of Paris 6, France, 1995). He undertook post-doctoral studies on infrared spectroscopic studies of hydrocarbons and the development algorithms for the detection of extrasolar planets using correlation techniques. Yves actual research interests concern the spectroscopy and kinetics of reactive intermediates and stable organic compounds of importance for Titan and the cometary environment.

François Raulin got a diploma from the Ecole Suprieure de Physique et Chimie Industrielles de la Ville de Paris in 1969, and a Doctorat d'Etat on prebiotic chemistry from the Universit Paris 6 in 1976. He is Full Professor at University Paris 12, and head of PCOS (Space Organic Physical Chemistry) group of LISA, he was director of which until 2005. His researches are related to planetology and exo/astrobiology, especially to Titan, comets and Mars. He is InterDisciplinary Scientist of the Cassini–Huygens mission and co-investigator of its CIRS (Cassini), ACP and GC–MS (Huygens) experiments. He is CoI of the COSAC and COSIMA experiments of the Rosetta European cometary mission. He is chair of COSPAR Commission F (Life Sciences), vice chair of COSPAR Planetary Protection Panel and first vice-president of ISSOL. He is also chair of the Exo/astrobiology working group of CNES. He is the author of mores than 250 scientific papers, and 9 books related to the field of the origins of Life and Exobiology.

1. Introduction

Further enlightened by the recent findings of the international space mission Cassini–Huygens, photochemistry of Titan's atmosphere has been arising in recent years an ever-increasing interest explained by the manifold importance of its most abundant minor constituent and most important photochemically active species, methane (CH_4). Driven by its photodissociation at Lyman α generating highly reactive radical species associated to a dense background N_2 atmosphere, a complex and multiphasic organic chemistry is indeed flourishing, possibly even reminding of some processes of our prebiotic Earth's environment [1]. Despite the quality of numerous investigations dedicated to this issue [2–7], theoretical models of Titan's atmosphere have however been unable to simultaneously fit the various observations. Although many microphysical and hydrodynamical models have been developed ever since [8,9] to apprehend the physical behavior of Titan's extensive haze, its chemical sources are still quite unknown [10,11] and the study of the important heterogeneous reactions it may induce in the atmosphere are only premises [12]. For that matter, Lebonnois [11] pointed out that the origin of the current discrepancies between computations and observations may lie in the adopted photochemical kinetic data itself.

Theoretical models of Titan's atmosphere require indeed a detailed, accurate description of all important reactions, photochemical processes, transport and constituents, relevant to its photochemistry. In order to build their photochemical schemes, underpinning of photochemical calculations, modelers base their arguments on photochemical reactions studied in the laboratory, amenable to experimental uncertainties, over a range of temperatures and pressures that are often not representative of Titan's atmospheric conditions. A major limitation in constructing accurate atmospheric models of the outer planets and their moons is especially the availability of low-temperature, low-pressure kinetic data, such as absorption cross sections, quantum yields and reaction rates. Indeed, most of the relevant experimental research has been motivated by the importance of hydrocarbon chemistry in combustion studies. The majority of published results describes therefore chemical systems different from the ones that can be found in the stratosphere of Titan, where appropriate conditions are $T = 71$–$175\,K$, $P < 0.2\,Torr$ and N_2 as background atmosphere. Most photochemical reaction rate coefficients have scarcely been determined in a temperature range representative of Titan's atmosphere, and their extrapolation to such low temperatures is therefore uncertain. For many recombination reactions moreover, only the high pressure limiting rate constants are available and the buffer gas is almost never N_2 as it should be for simulating Titan's chemistry. The identities of product species are finally rarely determined along with the measurements of kinetic rate constants nor are quantum yields for formation of neutral product species often reported when photodissociation cross sections are published. Literature, when available, sometimes offer estimates based on various chemical arguments but it is important however to keep in mind the nat-

ural tendency to use photochemical rate constants allowing the model to best match the data.

Every model can only be as good as the input data. The current accuracy of overall laboratory rate coefficients is estimated to be ∼20% [13]. However, for such strongly non-linear, heavily coupled systems as these photochemical models are, more precision than this may be required to produce accurate results. Many inquiries have already been devoted to estimate this overall precision in photochemical models of different planetary atmospheres [14–17] but none reported was however based on an extensive kinetic database representative of Titan's atmospheric conditions. They were rather based on already existing databases, however optimized for studying the Earth's atmospheric chemistry [18,19], combustion chemistry [20] or even astrochemistry [21]. Because of this lack of specific databases, studies dedicated to Titan's atmosphere have thus been inevitably restricted in their use.

In the following section of this paper, we therefore propose to review the photochemical reactions that are supposed to be the most important in Titan's atmosphere with a special emphasis on the processes that are still not well represented in the models. Enclosed qualifying statements are reported as a way of testifying to some extent the overall uncertainties in a reaction model representative of Titan's atmospheric photochemistry, while paying a particular attention to rely on the latest and/or more reliable experimental data available in the literature, insofar as conflicting conclusions had been raised previously. Following this comprehensive cross-examination of extensive databases, we propose afterwards some clues as for quantifying these photochemical sources of uncertainties and evaluating them for conditions representative of Titan's atmosphere, in order to enclose them easily in future calculations.

2. Photochemical sources of uncertainties in Titan's atmosphere modeling

Yung et al. [2] model provided the first major review of the laboratory, and theoretical, kinetics and photochemistry literature available at that time representing the largest compilation to date of chemical processes occurring in reducing planetary atmosphere. The chemical scheme displayed in Tables 1 and 2 reflects our own review of the laboratory measurements that have become available since Yung et al. [2] model. Several key reviews/compilations of laboratory photolysis and kinetic measurements provided useful information on reactions that may have been extensively updated, including Okabe [22], Tsang and Hampson [23], Tsang [24]; Baulch et al. [25,26]; these works are referenced in these tables where appropriate. Tables 1 and 2 consist of several types of chemical reactions whose rate constants may have been extensively updated: (a) photodissociation ($AB + h\nu \rightarrow A + B$), (b) insertion/H-atom substraction ($A + BH \rightarrow AB + H$), (c) H-atom abstraction ($A + BH \rightarrow AH + B$), (d) combination ($A + B \rightarrow AB$) and disproportionation ($A + A \rightarrow B + C$), (e) exchange and transfer ($A + BC \rightarrow AB + C$), and (f) cracking and/or H-atom scavenging ($A + H \rightarrow AH$, followed by $AH + H \rightarrow C + D$and/or $AH + H \rightarrow A + H_2$). Yung et al. [2] model and subsequent models of outer planets hydrocarbon photochemistry we founded part of our investigation on [3,4,27,6,10,7,11] present an extensive discussion of these reaction categories and their importance in the hydrocarbon chemistry of Titan's atmosphere, which will not be repeated here. In the following, we rather propose to review the photochemical sources of uncertainties among these reactions, whose knowledge may be an important prerequisite when modeling Titan's atmosphere.

2.1. Photochemistry of hydrocarbons

2.1.1. Direct dissociation of methane and its subsequent chemistry

Photochemistry of hydrocarbons in Titan's atmosphere is principally driven by methane (CH_4) photodissociation, occurring in the high atmosphere at VUV wavelengths for $\lambda <$ 145 nm, even though only 4.5 eV are needed to break it apart. Approximately 75% of methane absorption of radiation above 700 km is due to the intense solar Lyman α line at 121.6 nm. The primary dissociation channels energetically accessible at this wavelength are (adapted from [28]):

$$CH_4 + h\nu\,(\text{Lyman}\,\alpha) \rightarrow CH_3 + H \quad \text{(J1a)}$$

$$\rightarrow {}^1CH_2 + H_2 \quad \text{(J1b)}$$

$$\rightarrow {}^3CH_2 + H + H \quad \text{(J1c)}$$

$$\rightarrow {}^1CH_2 + H + H \quad \text{(J1d)}$$

$$\rightarrow CH + H_2 + H \quad \text{(J1e)}$$

In spite of having been extensively studied, the accurate yields of the different CH_4 photodissociation pathways, particularly at Lyman α, are still unresolved. To illustrate the full extent of this argument, as critically reviewed in Romanzin et al. [29], Table 1 displays different methane photodissociation pathways at Lyman α both experimentally investigated and implemented in previous Titan's photochemical models. Such significative incidence on the hydrocarbon chemistry of Titan's atmosphere was somewhat sensitivity-tested in Wilson and Atreya [7]. While the abundances of simple hydrocarbons such as acetylene (C_2H_2) and ethylene (C_2H_4) were not sensitive to the choice of methane photolysis scheme, minor C_3 molecules abundances showed substantial sensitivity in their abundances, especially propylene (C_3H_6) and propyne (methylacetylene) (CH_3C_2H) whose variations are even surpassing observational uncertainties. This confirms the obvious role performed by the primary radicals produced from methane (CH_4) photodissociation (CH_3, $^1CH_2$, $^3CH_2$ and CH) in the formation of heavier hydrocarbons. Concerning Lyman α photolysis, future models may follow the recommendations of the most recent and forefront experiment performed by Wang et al. [30] who, by means of multiple experiments, succeeded in drawing up a whole and coherent set of branching ratios.

Methane (CH_4) temperature-dependent photoabsorption cross sections from their absorption thresholds to 120 nm and at Titan's atmospheric temperatures, either are poorly known or not measured at all. The existing data were mainly reported

Table 1
Relative contributions of the CH_4 dissociation product channels after photoexcitation in the Lyman- α wavelength region (adapted from [29])

	J_{3a}	J_{3b}	J_{3c}	J_{3d}	J_{3e}
Experimental determinations					
Mordaunt et al. [155][a](scenario 1)	0.51	0.24	0.05 + *0.20*		0.00 + *0.00*
Mordaunt et al. [155][a](scenario 2)	0.49	0.00	∼ 0+ ∼ *0*		0.28 + *0.23*
Heck et al. [156]	0.66	0.22	∼0		0.11
Brownsword et al. [157]	0.38	0.52	0.01		0.08
Wang et al. [30]	0.291	0.584	–	0.055	0.07
Photochemical models					
Yung et al. [2]	0.00	0.41	0.51	0.00	0.08
Toublanc et al. [3] (scenario 1)	0.51	0.24	0.25	0.00	0.00
Toublanc et al. [3] (scenario 2)	0.49	0.00	0.00	0.00	0.51
Lara et al. [4]	0.49	0.00	0.00	0.00	0.51
Romani [158]	0.41	0.28	0.21	0.00	0.10
Dire [5]	0.67	0.22	0.00	0.00	0.11
Smith and Raulin [159]	0.41	0.53	0.00	0.00	0.06
Lebonnois et al. [6] (scenario 1)	0.49	0.00	0.00	0.00	0.51
Lebonnois et al. [6] (scenario 2)	0.41	0.53	0.00	0.00	0.06
Wilson and Atreya [7]	0.41	0.28	0.21	0.00	0.10
Hébrard et al. [17]	0.291	0.584	0.00	0.055	0.07

[a] The figures in italic correspond to $CH_4 + h\nu \rightarrow CH_3{}^* + H \rightarrow {}^{3,1}CH_2 + 2H$ for (J_{3c}) and (J_{3d}) and $CH_4 + h\nu \rightarrow CH_3^* + H \rightarrow CH + H_2 + H$ for (J_{3e}). These sequential contributions must be added to the direct contributions.

in the 1950–1970 decades and are almost exclusively available only at room temperature. Limited low-temperature CH_4 photoabsorption cross-section data were first reported by Mount and Moos [31] in the 138–160 nm region at 200 K. Most recently, Lee et al. [32] reported room temperature cross-section data of several methane (CH_4) isotopomers in the 105–145 nm region, with extreme care about the purification of impurities in the gaseous samples. Using synchrotron radiation as a continuum light source, Chen and Wu [33] measured methane (CH_4) absolute photoabsorption cross sections in the VUV–UV region at three different temperatures, i.e., 370, 295, and 150 K. Their methane (CH_4) cross-section values in the 120–142.5 nm region at 295 K agree well with previously reported values [34,35,32] with only ±10% evaluated experimental errors in absolute cross section values. Under these low-temperature conditions, Chen and Wu [33] found that methane CH_4 cross-section values increase in the short wavelength region and decrease in magnitude in the long wavelength region. In contrast to this behavior, the cross-section data obtained at high temperature show a relative decrease in the short wavelength region and a relative increase in the long wavelength region. The trends exhibited appear to be quite reasonable with Mount and Moos [31] reported results at 200 K. However, further measurements at temperatures between 295 and 150 K would be needed so that the temperature-dependent cross-section values can be theoretically modeled.

The lifetime of the excited state of methylene ($^1CH_2$) is very short since it is efficiently quenched down to the ground state methylene ($^3CH_2$) by collision with another atmospheric molecule [36]:

$$^1CH_2 + M \rightarrow {}^3CH_2 + M \quad (M = N_2 \text{ or } CH_4) \qquad (H1)$$

Excited methylene ($^1CH_2$), as well as methylidine radicals (CH), can also react with methane (CH_4) to form methyl radicals (CH_3) and ethylene (C_2H_4), respectively.

$$^1CH_2 + CH_4 \rightarrow CH_3 + CH_3 \qquad (H2)$$

$$CH + CH_4 \rightarrow C_2H_4 + H \qquad (H3)$$

The rate coefficients of reactions concerning the methylidine radical (CH), such as $CH + CH_4$, $CH + C_2H_2$, $CH + C_2H_4$ and $CH + C_4H_8$ reactions, were measured by Canosa et al. [37] in a temperature range of 23–295 K using the CRESU apparatus coupled with a pulsed laser photolysis-laser induced fluorescence (PLP-LIF) technique. This study confirmed the previous results of Berman [38,39], broadening them to temperatures more relevant for Titan's atmosphere without however giving any clear identification of the resulting products. Yet, their thermochemical and kinetic analysis advocated accordingly for the same H-atom abstraction process, which has experimentally been confirmed later by Fleurat-Lessard et al. [40] for the $CH + CH_4$ reaction and by McKee et al. [41] for the $CH + C_2H_2$ and $CH + C_2H_4$ reactions. Concerning the $CH + C_2H_6$ reaction, McKee et al. [41] conclusions are consistent with a competition between H-abstraction and CH_3-abstraction processes. Considering for the first time these formation mechanisms for methylacetylene (CH_3C_2H) and allene (CH_2CCH_2) in a photochemical model, Wilson and Atreya [7] assumed them to be both equally plausible quite satisfyingly even if Galland et al. [42] determined by VUV resonance fluorescence an absolute H-atom production equal to 22% using as reference the H production from the $CH + CH_4$ reaction. Wilson and Atreya [7] assumed also the same branching ratio for both C_3H_4 isomers, methylacetylene (CH_3C_2H) and allene (CH_2CCH_2), issued from the $CH + C_2H_4$ reaction.

Ground state methylene ($^3CH_2$) and methyl (CH_3) mainly react together to form ethylene (C_2H_4):

$$^3CH_2 + CH_3 \rightarrow C_2H_4 + H \quad \text{(H4)}$$

Ethane is mostly created in the atmosphere through methyl (CH_3) recombination.

$$CH_3 + CH_3(+M) \rightarrow C_2H_6\,(+M) \quad \text{(H5)}$$

Planetary emissions of the methyl radical (CH_3) were first observed in 1998 [43,44] by the infrared space observatory (ISO) in the upper atmospheres of Saturn and Neptune. Methyl radical (CH_3) is produced by VUV photolysis of methane (CH_4) and is a key photochemical intermediate leading to complex organic molecules in outer planetary atmospheres. Indeed, the methyl recombination reaction $CH_3 + CH_3 \overset{M}{\rightarrow} C_2H_6$ is of prime importance in photochemical modeling of Titan's atmosphere since it is the main source of ethane production. Until recently, its rate constant has been mostly measured as low as room temperature, and at high pressure in non-representative bath gases. The most widely adopted Slagle et al. [45] rate expressions for low-pressure, three-body limiting rate constant k_0 and high-pressure, two-body limiting rate constant k_∞ had to be extrapolated down to lower temperatures according to their own Arrhenius law, for use in atmospheric models of outer planets' atmospheres. Methyl (CH_3) abundance observed by ISO was however unexpectedly lower than predicted by photochemical models using this specific chemical rate value, specially in Saturn's atmosphere. An underestimation of the loss of methyl (CH_3) has thus been suggested in these models [43,44,46,27,47], which was thought to be mostly due to the poorly extrapolated rate constant at the low temperatures and pressures of these atmospheric systems. A prevailing remedy was then to increase the methyl (CH_3) recombination reaction measured at room temperature in rare gases by at least one order of magnitude, but within the range of disagreeing theoretical expressions when extrapolated to low temperature [48,45,49]. Cody recently reported studies at $T = 155$, 202 and 298 K and $P = 0.6$, 1.0 and 2.0 Torr He, using a discharge-flow reactor apparatus coupled to a quadrupole mass spectrometer (DF-MS), providing the first measurements of the methyl (CH_3) recombination rate constant in the fall-off region at $T < 296$ K [50,51]. Their conclusions were in agreement with the calculations by Klippenstein and Harding [52] on the pressure dependence of the methyl (CH_3) recombination reaction at $T = 200$ K when converted from M = Ar to M = He. The latest Wang et al. [53] experimental and theoretical investigations with He bath gas using time-resolved time-of-flight mass spectrometry (TOF-MS) and transition state theory (TST) are in very good agreement with Cody experimental data points at low-temperature and high-pressure limit [50,51]. In spite of these recent measurements, conducted with He as bath gas, Wilson and Atreya [7] still used a modified recombination rate that is ten times the Slagle et al. [45] expression, considering in addition that the reaction may proceed faster with Titan's N_2 background atmosphere as exhibited by the hydrogen atom recombination reaction k_0. However, merely the low-pressure, three-body limiting rate constant k_0 is proportional to the collision frequency and thus could be derived by using the appropriate reduced collision masses, Lennard–Jones collision cross sections as well as estimated values for the average energy transferred per collision ΔE. Following Smith [54] calculations, methyl (CH_3) recombination rate would proceed roughly 70% faster at low pressures in Titan's atmosphere. As Cody et al. [51] pointed out on the basis of these latest laboratory data, the remaining excess CH_3 predicted in the models relatively to the ISO observations may be explained to a large extent elsewhere in the CH_3 photochemistry and/or transport rather than in the $CH_3 + CH_3$ rate value. The exact reconciliation of this problem is beyond the scope of this paper but though, we preferred to stick to our general approach and to rely on the latest and most representative experimental data [53] rather than embrace the natural tendency to use chemical rate constants that allow the calculations to best fit the data.

Once ethylene (C_2H_4) is formed, it serves as a major source of acetylene through photolysis in the high atmosphere:

$$C_2H_4 + h\nu \rightarrow C_2H_2 + H_2 \quad \text{(J2a)}$$

$$\rightarrow C_2H_2 + H + H \quad \text{(J2b)}$$

Absorption cross sections of ethylene (C_2H_4) in the VUV region were first reported by Zelikoff and Watanabe [55], using a spectral bandwidth of ~0.1 nm. More recently, Cooper et al. [56] have reported the absolute photoabsorption cross-section of ethylene from 6 to 200 eV utilizing a high-resolution dipole (e, e) spectroscopy. Holland et al. [57] have measured the absolute photoabsorption, photoionization, and photodissociation cross sections of ethylene and deuterated ethylene from their ionization thresholds to 50 nm using a double ionization chamber technique and also include Zelikoff and Watanabe [55] and Cooper et al. [56] results in their compiled cross-section data. Before Wu et al. [58], there was no apparent temperature-dependent cross section measurements of ethylene available in the literature. Using synchrotron radiation as a continuum light source, Wu et al. [58] have measured temperature-dependent cross-sections of ethylene in the VUV 118–192 nm region at five different sample temperatures (370, 330, 295, 200, and 140 K). Their cross-section values measured at 295 K agree reasonably well with the Zelikoff and Watanabe [55] previously reported data except for larger cross-section values in the ~160–174 nm region, both at the absorption peaks and at the valleys, by as much as 15–20%. While it appears that these larger cross-section values at the absorption peaks result from the higher resolution used in Wu et al. [58] experiments, the reason for the positive discrepancy observed with Zelikoff and Watanabe [55] values at the absorption valleys still remains unclear. Because of the varying resolution inherent in the (e, e) spectroscopy technique adopted by Cooper et al. [56], it is harder to compare their data with Wu et al. [58] results without line shape convolution. Yet, it appears that the trend of their data is in good agreement with Wu et al. [58] results despite their bad contrast between peaks and valleys. Significant temperature effects were observed in the region between 170 and 192 nm, especially in the positions of the known hot bands, which appear to be enhanced at 370 K and significantly reduced at 140 K. The magnitude of temper-

ature effects on absorption cross sections of C_2H_4 decreases as a function of decreasing wavelength in the studied spectral range.

2.1.2. Dissociation of methane photocatalysed by acetylene

Laboratory experiments of irradiation at 185 nm of a mixture composed of CH_4 and C_2H_2 in catalytic proportion confirmed that the dissociation of methane could be catalysed by the photolysis of acetylene at lower altitudes [59]. Since the solar flux increases rapidly from 100 to 230 nm, this photocatalysed destruction of methane CH_4in the stratosphere can be significantly more important than its direct photolysis at high altitude:

$$C_2H_2 + h\nu\,(< 235\,\text{nm}) \rightarrow C_2H + H \quad \text{(J3a)}$$

$$\rightarrow C_2 + H_2 \quad \text{(J3b)}$$

Diatomic carbon (C_2) and ethynil (C_2H) radicals can then destroy methane (CH_4) to form CH_3radicals and regenerate acetylene (C_2H_2):

$$C_2 + CH_4 \rightarrow C_2H + CH_3 \quad \text{(H6)}$$

$$C_2H + CH_4 \rightarrow C_2H_2 + CH_3 \quad \text{(H7)}$$

Existing data were mainly reported in the 1960–1980 decades but were almost exclusively available at room temperature. The first photochemical models of Titan's atmosphere have inevitably used some of these data: Nakayama and Watanabe [60] data in the 106–180 nm region by using a spectral bandwidth of ~0.1 nm, Suto and Lee [61] data in the 106–180 nm region using a 0.04 nm bandwidth, and Seki and Okabe [62] data above 205 nm but at rather low resolution (1 nm bandwidth). Limited low-temperature acetylene (C_2H_2) cross section data were first reported by Wu et al. [63] in the 154–193 nm region and later extended by Chen et al. [64] to 215 nm at 155 K, by Smith et al. [65] in the 147–201 nm region at 195 K and by Bénilan et al. [66] in the 185–235 nm region at 173 K. Wu et al. [63], Chen et al. [64] and Smith et al. [65] argued for the presence of hot bands whose intensities decrease when the temperature decreases. From spectroscopic measurements and thermodynamic studies, these earlier data were however shown to be contaminated with the acetone absorption features at 190 and 195 nm [67]—commercially used as a chemical stabilizer. As its absorption bands are 100 times more intense than those of acetylene in the same wavelength range, the presence of less than 1% acetone in the samples was enough to explain the observed variations. The acetone contamination was effectively eliminated in Wu et al. [68] data at 155 K and [66] data at 173 K by employing standard purifying procedures since the melting point of acetone is 180 K. As Wu et al. [68] pointed out that the absorption spectra in this spectral region often exhibit very sharp features, they advocated that high-resolution and low-temperature cross-sections measurements would be needed in order to provide spectral identification and cross-section data for the accurate determination of abundances and temperature profile of planetary atmospheres. Bénilan et al. [66] observed no decrease of the photodissociation coefficient with the spectral resolution (less than 1% between 0.02 and 2 nm resolutions), thus demonstrating that there should be no need for high resolution absorption cross-sections to calculate photodissociation coefficients in photochemical models.

A number of experiments were performed in order to determine primary quantum yields for product formation following acetylene (C_2H_2) photodissociation at various wavelengths (193.3 nm [69,70,62], 184.9 nm [71], 147.0 nm [72] and 123.6 nm [73]). The results of these studies, which were mainly performed employing static sample photolysis along with stable end-product analysis [62,71,72], indicated that the quantum yield for the simple C–H bond fission channel $H + C_2H$ is only 0.1–0.3 (see Table 1 in [62]) and it was tentatively suggested that the major primary photochemical process was the formation of an electronically excited metastable acetylene ($C_2H_2^*$) [62,74] and/or vinylidene (H_2CC^*) [75]. As further state-resolved dynamics studies performed to investigate the primary photofragmentation dynamics of this $H + C_2H$ product channel in the ground-state could not find any indication for the formation of these metastable states [76,77], serious doubts concerning the validity of these low values reported in the literature so far were raised. Acetylene (C_2H_2) dissociation dynamics after photoexcitation at 193.3 nm and at the Lyman-α wavelength (121.6 nm) were then studied under collision free conditions by Lauter et al. [78] who, by obtaining absolute quantum yields for H atom formation close to unity, proposed that ethynyl (C_2H) radicals may indeed dominate the acetylene (C_2H_2) primary dissociation for both photolysis wavelengths rather than any "nonreactive" electronically excited metastable state of acetylene ($C_2H_2^*$) and/or vinylidene (H_2CC^*).

2.1.3. Formation of higher hydrocarbons

Methane (CH_4) and acetylene (C_2H_2) photolysis lead to a large panel of radicals reacting among themselves to produce heavier species. Titan's photochemistry can be thus considered as a succession of initiation, propagation and termination reactions.

The initial step is the formation of radicals by photodissociation of stable molecules or by additions of hydrogen atoms on unsaturated compounds in the presence of a third body (combination):

$$CH_4 + h\nu \rightarrow CH + H_2 + H \quad \text{(J1e')}$$

$$C_2H_2 + h\nu \rightarrow C_2H + H \quad \text{(J3a')}$$

$$C_2H_4 + H(+M) \rightarrow C_2H_5\,(+M) \quad \text{(H8)}$$

The second step is the propagation of the chain by the attack of a radical on a stable molecule by H-abstraction or insertion/H-substraction. In the last case, the molecule is necessarily an unsaturated one:

$$C_2H + C_2H_6 \rightarrow C_2H_2 + C_2H_5 \quad \text{(H9)}$$

$$C_2H + C_2H_2 \rightarrow C_4H_2 + H \quad \text{(H10)}$$

Finally, the chain ends when a radical reacts with another radical or with a stable molecule in a disproportionation or a combination reaction. The latter always involves a third body

and is therefore favored at high pressure:

$$CH + C_2H_4 \rightarrow CH_3C_2H + H \quad (H11)$$

$$CH + C_2H_4 \rightarrow CH_2CCH_2 + H \quad (H12)$$

$$CH_3 + C_2H_5(+M) \rightarrow C_3H_8\,(+M) \quad (H13)$$

Ethynyl radical, C_2H, is an abundant polyatomic species in interstellar space and is known to be important in Titan's atmosphere, where it is one of the important species responsible for the synthesis of higher hydrocarbons [2–4]. Produced by direct photolysis of acetylene (C_2H_2), the ethynyl radical (C_2H) indeed initiates the production of saturated hydrocarbons (C_2H_6, C_3H_8,. . ., C_nH_{2n}) through the indirect UV photolysis of methane (CH_4).

Until recently, reactions involving ethynyl radicals and several hydrocarbons have been studied down to 150 K using a cryogenically cooled flow cell combined with transient IR laser absorption spectroscopy (PLP-IrAbs(C_2H)) [79–82]. Low-temperature kinetics measurements lower than 150 K were recently reported, carried out with a CRESU apparatus or a pulsed Laval nozzle apparatus employing a pulsed laser photolysis-chemoluminescence technique (PLP-CL(CH^*)) [83–87]. Murphy et al. [87] computed activation energies are in quite good agreement with Ceursters et al. [88] ab initio calculations, advocating for a direct H-atom abstraction mechanism for ethynyl C_2H + alkane reactions. Concerning ethynyl(C_2H) + acetylene (C_2H_2) and ethynyl(C_2H) + alkene reactions, Chastaing et al. [83] measurements and thermochemical considerations point towards an overall indirect H-atom substitution process via an initial formation of an energized complex. Reaction $C_2H + C_2H_4$ is thought to significantly contribute to the ethene (C_2H_4) destruction rate. There have been however obvious difficulties in reproducing the observed ethene abundance in Titan's atmosphere despite these latest laboratory data. Toublanc et al. [3] model significantly underestimates the ethene abundance compared to the Voyager IRIS observation data by using a rate constant underestimated by almost an order of magnitude (2.5×10^{-11} cm^3 molecule^{-1} s^{-1}, based on Tsang and Hampson [23] estimation). But Lebonnois et al. [6] and Wilson and Atreya [7] models underestimate it too, even by using Opansky and Leone [82] rate constant whereas Lara et al. [4] calculations reproduce well the ethene (C_2H_4) abundance without even including the reaction in their chemical scheme but rather by assuming synthetically a flux from the surface, resulting from some surface processes. Wilson and Atreya [7] advocated for a possible irradiation of hydrocarbon condensates on Titan's surface as a source of ethene (C_2H_4) in the stratosphere. It seems however that these unique inconsistencies exhibited by ethene (C_2H_4) abundance may be the direct consequences of a peculiar coupling between its chemistry and its vertical transport (Lebonnois, personal communication).

2.1.4. Formation of polyynes

Polymerization of acetylene (C_2H_2) through polyyne formation has been postulated for the formation of solid organic material and thus for the creation of haze particles in the atmosphere of Titan [89]. As ethynyl radicals (C_2H) proceed to react with subsequently formed molecules, the process may continue, forming everincreasingly large successive polyacetylene polymers: triacetylene (C_6H_2), tetraacetylene (C_8H_2), etc. While triacetylene (C_6H_2) has not yet been identified in the atmosphere of Titan, laboratory simulations in Titan-like conditions (100–150 K) have however detected it [90]:

$$C_{2n}H_2 + h\nu \rightarrow C_{2n}H + H \quad (J3an)$$

$$C_{2n}H + C_{2m}H_2 \rightarrow C_{2(n+m)}H_2 + H \quad (H10n)$$

Polyynes chemistry remains however poorly understood as our current knowledge on the building of complex long-chain carbon compounds from simpler hydrocarbons comes only from pyrolysis processes at high temperatures and soot production [91,92]. As there is unfortunately little published on the rate coefficients involving polyyne species larger than C_2H_2either under the conditions of Titan or even at ambient temperature (see Table 2), the only way for modelers to include these reactions in their chemical scheme is to evaluate their rate coefficients from similar reactions rates available in the literature. Assuming that larger polyacetylene radicals may be less reactive than ethynyl radical ($C_{2n}H$), Yung et al. [2] adjusted arbitrarily their rate coefficient according to $k(C_{2n}H) = 3^{1-n}k(C_2H)$. Wilson and Atreya [10] adopted preferably the assumption that all H-atom abstraction reactions forming $C_{2n}H_2$ from $C_{2n}H$ and all reactions leading to $C_{2n}H_2$ had rate constants equal to the comparable reactions where $n = 1$.

Diacetylene (C_4H_2) absolute photoabsorption cross sections values determined recently between 120 and 180 nm by Okabe [72] were found to suffer from saturated experimental conditions which could have strongly influenced the subsequent published coefficients. Future modelers would be wise to adopt Kloster-Jensen et al. [93] cross sections instead, whose relative intensities can be easily fitted from Fahr and Nayak [94] absolute photoabsorption coefficients at 1645 Å. As this higher photoabsorption cross section leads to a lower stability towards

Table 2
Review of available experimental parameters relevant to polyynes chemistry (adapted from [98])

Parameter	Reaction	Available data	Improvements
Absorption coefficient	$C_{2n}H_2 + h\nu$	$n = 1, 2, 3$ (200 K) $n = 4$ (300 K)	Low temperature and low pressure
Quantum yield	$C_{2n}H_2 + h\nu$	$n = 1, 2$	Dependence on wavelength
Kinetic rate constant	$C_{2n}H + C_{2m}H_2$ $C_{2n}H_2{}^* + C_{2m}H_2$	$n = m = 1$	Low temperature and low pressure
Radiative lifetime	$C_{2n}H_2{}^*$	$n = 1, 2$	Low temperature

photochemical loss, diacetylene (C_4H_2) would have a shorter lifetime in Titan's atmosphere than indicated by previous models which have underestimated its photolysis rate. Most of these models have consequently tended to predict larger amounts of diacetylene (C_4H_2) than observed. An improved photolysis of diacetylene (C_4H_2) may also increase the predicted abundances of the heavier polyynes in photochemical models.

Along with polyacetylenic radicals ($C_{2n}H$), metastable diacetylene ($C_4H_2^*$) may also contribute to the long-chain polyynes species chemistry in Titan's atmosphere [95,96]. Resulting from diacetylene (C_4H_2) absorption of ultraviolet radiation at wavelengths well below the dissociation threshold, its relaxation can occur not only through intrinsic radiative and non-radiative decays but through collisions with other molecules as well. Determining precisely the lifetime of $C_4H_2^*$ is capital since a longer lifetime would give more time to $C_4H_2^*$ to react with other hydrocarbons to produce heavy compounds. Before any experimental data for the radiative lifetime of $C_4H_2^*$ was available, previous models assigned to it arbitrarily the lowest limit value determined for excited acetylene ($C_2H_2^*$) (1 ms) calculated by Lisy and Klemperer [97]. Lebonnois et al. [6] however had to lower this arbitrary relaxation rate by a factor of 5000 to reach agreement with Voyager observations. Using a low temperature matrix isolation technique, Vuitton et al. [98] recently performed the first direct measurement of the intrinsic lifetime of $C_4H_2^*$ and determined it to be of the order of 100 ms.

Photodissociation quantum yields of polyynes higher than diacteylene (C_4H_2) have never been determined, and neither have the photoabsorption cross sections of those higher than tetraacetylene (C_8H_2), at least in gas phase. Semi-empirical calculations performed in order to obtain absorption cross sections of higher polyynes tend to prove that the dissociation coefficient of any polyynes increases with its size [99].

The major production pathway for benzene formation appears to be propargyl (C_3H_3) radicals recombination:

$$C_3H_3 + C_3H_3 + M \rightarrow C_6H_6 + M \quad \text{(H14)}$$

The determination of this reaction rate and its associated branching ratios under various experimental conditions is also expected to be significant in evaluating the role of this radical in the formation of polyaromatic hydrocarbons in Titan's atmosphere. Fahr and Nayak [100] have determined the product yields and rate constants for propargyl radical (C_3H_3) combination reactions at 298 K by employing excimer laser photolysis in conjunction with GC–MS product analysis methods. Their rate constant is in relatively good agreement with the one derived from Alkemade and Homann [101] studies in the 623–673 K temperature range by using a low-pressure flow reactor and nozzle beam mass spectrometric product detection and analysis method. Using real-time infrared absorption spectroscopy, Morter et al. [102] however measured a significantly faster rate constant for propargyl (C_3H_3) self-reaction at 295 K. At this time, nothing is certain about the source or sources of discrepancies between the rate constant values reported by these different studies, and there is still no way to validate Fahr and Nayak [100] isomeric yields.

Lebonnois [11] has conducted sensitivity studies of benzene and PAHs formation both for Titan and Jupiter, testing these experimental data in different photochemical schemes, for which the modeled composition fairly agrees with observational constraints. Their results show that the uncertainties discussed above for several key reactions in benzene's production scheme are not of first order significance and that benzene abundance is mainly sensitive to some other reactions that may affect the propargyl (C_3H_3) radical.

2.2. Photochemistry of nitriles

Nitrile compounds formation is initiated in Titan's reducing atmosphere by N_2 dissociation, proceeding mostly through direct EUV photolysis and galactic cosmic ray (GCR) absorption [4]. With their refined treatment of UV (80–100 nm), EUV (<80 nm), soft X-rays (<5 nm) and photoelectrons (<80 nm)-induced N_2dissociation based on several experimental references, Lara et al. [103] found the $N(^2D)$ and $N(^4S)$ total production rates to be very similar at all altitudes, although the partial contributions from solar radiation (>80 nm) and photoelectrons (<80 nm) are somewhat different. Nitrogen N_2 also undergoes electron-impact dissociation, with quantum yields determined by Zipf and Gorman [104] and Itakawa et al. [105]. At lower altitudes, the main source of atomic nitrogen is provided by cosmic ray-induced dissociation, treated with or without neglecting the entire cascading energy deposition developed by Capone et al. [106]. Effect of magnetospheric electrons, magnetospheric protons and interplanetary electrons was proposed too as potential source for dissociating N_2[107] but appeared recently to be negligible as supported by Toublanc et al. [3] theoretical calculations.

Subsequently formed atomic nitrogen species ($N(^2D)$, $N(^4S)$, N^+) combine then with hydrocarbons to form an assortment of nitrile neutrals and ions in the upper atmosphere. Hydrogen cyanide HCN, the basis of nitrile chemistry, is thus formed through photodissociation, electron impact processes and photoionization.

Since the quenching of $N(^2D)$ by N_2 is not efficient, $N(^2D)$ reacts mostly with methane (CH_4) and ethylene (C_2H_4):

$$N(^2D) + CH_4 \rightarrow CH_2NH + H \rightarrow NH + CH_3 \quad \text{(N1)}$$

$$N(^2D) + C_2H_4 \rightarrow CH_3CN + H \quad \text{(N2)}$$

The recommended $N(^2D) + C_2H_4$ reaction rate constant values at 298 K and its associated temperature coefficients [108] are based on previously reported values [109–111]. Umemoto et al. [112] recently reported the yields of NH and H to be 0.3 and 0.8, respectively, confirming the insertion mechanism previously advocated for from ab initio calculations [113,114].

Sato et al. [115] measured $N(^2D) + C_2H_4$ reaction rate down to 230 K and obtained a rate value 20 times over what was previously estimated by Lellouch et al. [116] and Lara et al. [4] on the basis of $N(^2D)$ quenching coefficients measured by Black et al. [117]. Furthermore, crossed-beam experiments conducted by Balucani et al. [118] indicated acetonitrile (CH_3CN) to be indeed the likely product.

Dissociation of hydrogen cyanide (HCN) and all other nitriles yield the cyano CN radical, which can react with various hydrocarbons to maintain the CN bond.

$$HCN + h\nu \rightarrow CN + H \quad (J4)$$

Jolly et al. [119] review showed a critical lack of data concerning the photoabsorption coefficient available in the vacuum ultraviolet domain (110–210 nm) for N-organic molecules present or expected to be present in Titan's atmosphere. In particular, many absorption cross-sections have never been measured at low temperature. This lack is even greater for molecules not commercially available since, even at room temperature, absolute absorption coefficients are not available or erroneous. Therefore, they designed a new specific technique using synchrotron facility to measure the absorption cross sections in the VUV range at the low temperature range characteristic of Titan's atmosphere and adopted it first to study hydrogen cyanide (HCN), cyanoacetylene (HC_3N) and cyanodiacetylene (HC_5N):

$$CN + CH_4 \rightarrow HCN + CH_3 \quad (N3)$$

$$CN + C_2H_2 \rightarrow HC_3N + H \quad (N4)$$

$$CN + C_2H_4 \rightarrow C_2H_3CN + H \quad (N5)$$

Lara et al. [4] suggested a source provided by $CN + CH_4$ and $CN + C_2H_6$ in order to explain the CH_3CN observations announced by Bézard et al. [120]. Previous low-temperature studies [121–123] give however no indication of an acetonitrile channel. Although Balla and Casleton [124] pointed out that though the acetonitrile (CH_3CN) channel may be thermodynamically possible, their measurements only indicate traces of it.

Sims et al. [123] studied the reactions of the cyano CN radical with methane (CH_4), acetylene (C_2H_2), ethylene (C_2H_4), ethane (C_2H_6) and propene (C_3H_6) at low and ultra-low temperatures using a pulsed laser-photolysis (RLP), time-resolved laser-induced fluorescence (LIF) technique coupled to a CRESU apparatus. Reactions of the cyano CN radical with methane (CH_4) and ethane (C_2H_6) were expected to occur directly and to involve exothermic abstraction of an H atom as supported by Copeland et al. [125] and Arunan et al. [126] infrared chemiluminescence observations of vibrationally excited HCN and Balla and Casleton [124] HCN observations through time-resolved diode laser absorption spectroscopy. Reactions between cyano CN radicals and simple unsaturated hydrocarbons, C_2H_2, C_2H_4, and C_3H_6 have rate constants close to simple collision theory values, showing a mild negative temperature dependence, and exhibiting no dependence on total pressure. The only rational explanation suggested by Sims et al. [123] for these observations is that reaction involves an addition-elimination mechanism resulting in exothermic displacement of an H atom by a CN radical. Sims et al. [123] results were the first kinetic data to be obtained for these reactions at temperatures typical of those of outer planetary atmospheres. Although these reactions may not have previously been thought of as important in such environment, their still fast reaction rates down to low temperatures gave Sims et al. [123] observations significant consequences for planetary atmospheres and interstellar clouds chemical modeling.

Knowledge of the nitriles chemistry is still to be improved. Cyanoethynyl radicals (C_3N) may behave in the same way as ethynyl radicals (C_2H), and their insertion in $HC_{2n+1}N$ molecules could be similar to the insertion on the $C_{2n}N_2$. Some preliminary studies showed that the reactivity of the excited state HC_3N^* could be high, and that it could react in a similar way to C_4H_2* [127].

2.3. Photochemistry of CO and CO_2

Stratospheric measurements of carbon monoxide CO [128–130], carbon dioxide (CO_2) [131–133] and water (H_2O) [132] have indicated the presence of an oxygen chemistry in Titan's atmosphere. An external water (H_2O) flux of 3–50 $\times$ 10^6 cm^{-2} s^{-1} [134] is usually adopted to account for the water influx arising most probably from micrometeorites ablation and initiating such chemistry. Water (H_2O) photodissociation by solar radiation occurs then essentially in the mesosphere and thermosphere from the first absorption band (140 nm $< \lambda <$ 190 nm) and from the solar Lyman α line at 1216 nm, yielding OH radicals, ground state oxygen atoms $O(^3P)$ and excited oxygen atoms $O(^1D)$:

$$H_2O + h\nu\,(\text{Lyman}\,\alpha) \rightarrow OH + H \quad (J5a)$$

$$\rightarrow O(^1D) + H_2 \quad (J5b)$$

$$\rightarrow O(^3P) + H + H \quad (J5c)$$

Excited oxygen atoms $O(^1D)$ quickly relax in the ground state $O(^3P)$ by collision with molecular nitrogen (N_2) and methane (CH_4), or by spontaneous relaxation. Thus, only OH and $O(^3P)$ have to be considered in order to explain the presence of carbon monoxide (CO) and carbon dioxide (CO_2) in Titan's atmosphere.

Three pathways were used in the models to explain the formation of CO from this external source of water (H_2O):

$$O(^3P) + {}^3CH_2 \rightarrow CO + 2H \quad (O1)$$

$$OH + {}^3CH_2 \rightarrow CO + H_2 + H \quad (O2)$$

$$OH + CH_3 \rightarrow CO + 2H_2 \quad (O3)$$

These mechanisms were first suggested by Samuelson et al. [135] as sources for carbon monoxide (CO) from an external water influx. However, no further laboratory studies [136,137] have detected it as a product of these reactions to confirm Fenimore [138] first measurements and validate such mechanisms. Lara et al. [4] suggested that carbon monoxide (CO) may be provided directly from influx of micrometeorites, although a typical cometary inventory would not provide enough influx to achieve equilibrium. Primordial CO still remains therefore the most likely source. Wilson and Atreya [7] nominal model calculated an upward CO flux of 3.9 $\times$ 10^6 cm^2 s^{-1} necessary to maintain photochemical equilibrium. They suggested that some surficial processes concerning carbon dioxide (CO_2) and/or formaldehyde (H_2CO), such as outgassing from the interior or irradiation

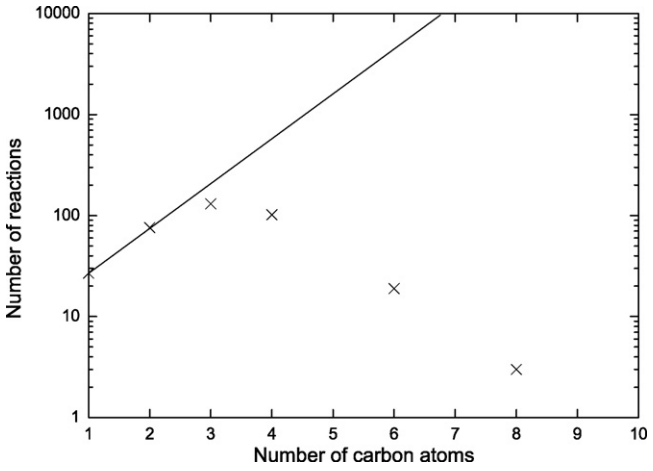

Fig. 1. Number of reactions considered in our chemical scheme of Titan's atmosphere plotted as a function of the number of carbon atoms in the considered species. The line shows the probable exponential law governing the number of reactions involving the smallest species.

of condensates, may provide another source for carbon monoxide CO. Following Wong et al. [139] postulate according which carbon monoxide (CO) may have been as much as 14 times more abundant after the initial escape stage in Titan's early evolution, Wilson and Atreya [7] pointed out the possibility that it may not be nowadays in equilibrium and was more abundant in Titan's past.

The formation of CO_2 is simply explained by the reaction of CO and OH:

$$CO + OH \rightarrow CO_2 + H \quad (O4)$$

CO is also engaged in chemical reactions mainly in the lower atmosphere, where it produces other oxygenated compounds through pressure-dependent reactions:

$$CO + {}^3CH_2 \rightarrow CH_2CO \quad (O5)$$

and

$$2(CO + H \rightarrow HCO) \quad (O6)$$

$$\frac{HCO + HCO \rightarrow H_2CO + CO}{CO + 2H \rightarrow H_2CO} \quad (O7)$$

2.4. Incompletion of chemical schemes

Furthermore, it is possible that critical reactions have never been studied and thus are not incorporated at all into the models, such omission of an important reaction may lead to misinterpretation of the results. Many more species and reactions may indeed exist than are explicitly considered in the chemical schemes, and that is already a source of systematic errors. These errors can tentatively be estimated by simply enumerating the different reactions according to the number of carbons in the parent compound, as described as crosses in Fig. 1. Despite the fairly limited number of species implemented in our chemical scheme, the total number of reactions generated to describe the full set of photochemical processes on Titan can be extremely large. According to Aumont et al. [140], this total number of reactions may follow an exponential distribution, with a growth factor depending on the different functionalities considered in our reacting species. Fig. 1 states that even if our reactions involving the smallest species may be governed by such kind of exponential law (continuous line), there is however an obvious and deep lack of information regarding the larger species. Even so, Vuitton et al. [141] recently showed that the photochemistry of the larger species has a preponderant role in determining the concentrations of the lighter species and that considering that these species are simply lost from the system could not be a valid assumption in future photochemical models of Titan's atmosphere.

3. Quantifying uncertainties on kinetics parameters

In general, a measurement procedure, either theoretical or experimental, has imperfections that give rise to a certain measurement error. Errors may be random or systematic. Random errors arise from unpredictable variations in measurements. Systematic errors, often called biases in measurements, are introduced by an imperfect knowledge of the values for known parameters, a faulty calibration or an intrinsic uncertainty attached to the technique used. Even if modern techniques are capable of measuring rate coefficients with an appreciable precision, data obtained in different laboratories on the same reaction using often the same technique are indeed rarely concordant to the extent that might be expected from the precision of the measurements. Besides, even if the spread in results among different techniques for a given reaction may provide some basis for evaluating an uncertainty, the possibility of the same, or compensating, systematic errors in all the studies must be however recognized and make them particularly difficult to detect and to quantify (Fig. 2).

In addition to the above detailed investigation of the photochemical sources of uncertainties in theoretical modeling, our goal was to provide a better evaluation of these uncertainties at temperatures representative of Titan's atmospheric conditions. Assigned uncertainties represent our own subjective assessment. Their determination does not result from a rigorous, statistical analysis of the database, which generally is too limited to permit such an analysis, but is rather based on an estimation of the difficulties of the experiments as well as their potential for systematic errors, seeking to identify the strengths and limitations of the different techniques with respect to their use at low temperatures.

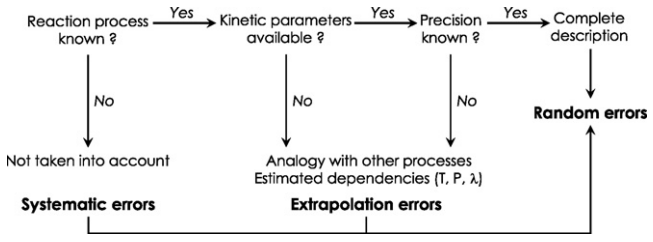

Fig. 2. Flow diagram of the main sources of uncertainties found in photochemical models.

3.1. Photodissociation rates uncertainty

Photodissociation rates $J_i(z)$ (s^{-1}) at the altitude z of the different absorbing species i included in the model can be computed in the range of wavelength $[\lambda_1, \lambda_2]$ as

$$J_i(z) = \sum_j \left(\int_{\lambda_1}^{\lambda_2} q_{i,j}(\lambda, T)\sigma_i(\lambda, T)F(\lambda, z)\,d\lambda \right) \quad (1)$$

which requires beforehand the determination of their absorption cross-sections $\sigma_i(\lambda, T)$, their different photodissociation pathways j characterized by quantum yields $q_{i,j}(\lambda, T)$ and the actinic flux at every level in the atmosphere $F(\lambda, z)$ as well. Specific inaccuracies in both photoabsorption cross-sections and quantum yields determination as well as imprecision carried by incident solar flux calculations result then inevitably in uncertainties in photolysis rates $J_i(z)$. The whole set of adopted nominal photodissociation parameters is displayed along with their uncertainty parameters in Table 1.

Uncertainties in both quantum yields and absorption cross sections are mostly due to a lack of accurate experimental determination. Photoabsorption cross-sections and quantum yields have indeed been investigated only at a few specific wavelengths and may thus be systematically underestimated. Different laboratory measurements could even diverge significantly and could consequently affect the results of photochemical models. To illustrate the full extent of these issues, we can refer to the still unresolved argument on methane photodissociation pathways at Lyman α critically reviewed in Romanzin et al. [29] or our foregoing comments on C_4H_2 absorption.

Due to this important lack of reliable data in the literature, several quantum yields have thus to be estimated along with their dependencies in wavelength as well as in temperature, while experimental uncertainties quoted in the literature are often considered already equal to 10%. The uncertainty factor F_q attached to the quantum yield $q_{i,j}(\lambda, T)$ cannot therefore be estimated to a high level of precision neither, and we classified them in our evaluation in only three categories of precision: within 10% ($F_q = 1.1$), 25% ($F_q = 1.25$) and 50% ($F_q = 1.50$).

Even if our knowledge of low-temperature UV photoabsorption cross sections for relevant hydrocarbons has improved greatly thanks to many available measurements [68,58,33,142,66,143,94,144,65], their temperature-dependency remain highly uncertain. Temperature-dependence of the UV photoabsorption cross sections may indeed vary significantly in many different ways according to the compound and the wavelength considered, and could differ by many orders of magnitude compared to room temperature values, a typical temperature for the measurements supplying the majority of cross-sections data. To illustrate the importance of this issue, acetylene (C_2H_2) and diacetylene (C_4H_2) cross-sections values were found to decrease respectively by as much as 40% between 295 and 150 K in the 120–240 nm region [58] and 50% between 293 and 193 K in the 195–265 nm region [143]. Fahr and Nayak [144] established moreover that methylacetylene (CH_3C_2H) cross section values remain nearly independent of temperature near the absorption peak at 172.4 nm, whereas they increase with increasing temperature at longer wavelengths. It would seem ideal to develop a theoretical model to allow modelers to interpolate and extrapolate the cross-section values over a desired temperature range, for example, down to about 100 K for application in the atmospheric conditions of Titan. However, Wu et al. [58] pointed out that these temperature effects could be more complicated than simple variations in the population distribution functions would imply. It is indeed not uncommon to find different electronic transitions, involving absorption from different vibrational modes of the ground electronic state, complicated by potential energy surface crossing, perturbation, predissociation and rovibronic coupling occurring in these molecular systems. According to Wu et al. [58], if feasible, such theoretical model could therefore be applied only over a certain spectral region, but not the whole spectral range.

According to the authors concerned, the mere evaluation of uncertainties in cross-sections from laboratory measurements is a difficult task and the value of the standard deviation is therefore not systematically given. Values however available in the literature are usually of the order of 10–25% [145,146,142,68,33,58]. In this review, we paid of course a particulate attention to rely on the photoabsorption cross sections at the lowest temperature available in a given wavelength range to evaluate their intrinsic uncertainties at temperatures and wavelengths representative of Titan's environment. For this evaluation, we took into account their absolute experimental uncertainties, when available, as well as our subjective estimation of their overall dependencies in temperature, their consistencies with other available data in their same limited spectral range and over the whole spectrum. In this way, the uncertainty factors F_σ we estimated range from 1.15 to 1.65, i.e., within 15–65% precision.

Finally, the actinic flux at every level in the atmosphere $F(\lambda, z)$ is usually calculated by a radiative transfer program which includes, among others, absorption and scattering by atmospheric species. The contribution of this calculation to the total imprecision carried by the incident flux is difficult to evaluate as it comes from model assumptions themselves, uncertainties in absorption and scattering cross-sections, uncertainties in quantum yields and uncertainties in compound distributions. Each of these factors taken alone should already modify significantly the calculation of $J(z)$; their combination would obviously worsen it a lot more. However, because of the feedback between the abundances and the photodissociation processes in the actinic flux calculation, these uncertainties would be difficult to evaluate without an extensive theoretical investigation beyond the frame of the present review. While usually extrapolated from values measured at maximum and minimum solar activity, photolysis rates should nevertheless be calculated in further publications for a solar activity corresponding to the time of the observations used for validating the theoretical results.

If we assume a standard deviation of 50% for quantum yields, 65% for absorption cross-sections and without considering any contribution from the radiative transfer model's own assumptions, we obtain a maximum standard deviation of about 250% for $J_i(z)$. NASA JPL (2003) recommended to use global uncertainty factors F_J in the range [1.3–3] which correspond to

standard deviations of photolysis rates in the range [30–300%]. The lower limit of 30% corresponds to combined uncertainties for cross-sections and quantum yields of well known terrestrial species like molecular ozone (O_3), hydrogen chloride (HCl) and principal chloro-(CCs) and chlorofluoro-carbon (CFCs) species. Compared to this Earth-based database, and taking into account the peculiarity of Titan's conditions and species, we consider that our adopted uncertainty estimations are well within what could be expected for such an environment.

3.2. Bimolecular and termolecular reaction rates

The rate coefficients for the three-body pressure dependent reactions ($cm^6\,s^{-1}$) are usually interpolated between the low-pressure, three-body limiting rate values k_0 ($cm^6\,s^{-1}$) and the high-pressure, two-body limiting rate values k_∞ ($cm^3\,s^{-1}$) with the semi-empirical Lindemann–Hinshelwood equation:

$$k(T, M) = \frac{k_0(T)k_\infty(T)[M]}{k_0(T)[M] + k_\infty(T)} \quad (2)$$

where $[M]$ is the total atmospheric density (cm^{-3}). More refined treatments of pressure effects in the falloff region have been suggested [147,148]; however introducing the additional parameters required by these more complicated expressions may enhance the overall chemical uncertainty of the model. Moreover, Gladstone et al. [149] have already demonstrated their minimal effects on the resulting concentrations of the major hydrocarbon compounds in their own model of Jupiter's atmosphere.

Modelers carefully choose their updated chemical rate coefficients according to their relevance to Titan's atmosphere conditions; thus by focusing their attention on the temperature, but also on the pressure and the bath gas used during the determination. Laufer et al. [150] and Yung et al. [2] discussed the application of theoretical and semiempirical techniques to estimate recombination reaction rate constants not otherwise measured in laboratory experiments. On the basis of considerations concerning transitory excited reaction intermediates and fast rate coefficients, Laufer et al. [150] suggested a scaling between the rate constants for several hydrocarbon reactions. However, merely the low-pressure, three-body limiting rate constant k_0 is proportional to the collision frequency and thus could be derived by using the appropriate computational technique involving reduced collision masses, Lennard–Jones collision cross sections as well as estimated values for the average energy transferred per collision ΔE. The different available approaches are semi-empirical in essence, in that parameters are adjusted within reasonable values to best match the data. Even the recommended rate constant derived from one of the most sophisticated and most reliable method, the Microcanonical variational transition state theory (MCVTST)/master equation, exhibit uncertainties in relative values likely up to 25–35% [54].

Moreover, reaction rates and their attached uncertainties are supposed to be constrained within the temperature range of their experimental and/or theoretical determination, which is often not representative of Titan's altitude-dependent temperatures. The UMIST99 database for astrochemistry[1] [21] provides such information, but for conditions representative of the interstellar medium and with a lower level of precision, as rate coefficients are classified in only four categories of precision: within 25%, 50%, 100% and 900%. NASA JPL panel data evaluation [18] or the International Union of Pure and Applied Chemistry (IUPAC) evaluation [19] are restricted to the 200–400 K temperature range, optimized as they are indeed for Earth chemistry (conditions, species). Baulch et al. [20] latest critical evaluation of kinetic data is restricted for combustion modeling and thus only for temperature above 298 K. Extrapolating these uncertainties at temperatures representative of Titan's atmospheric conditions constitutes however another source of uncertainty.

Stewart and Thompson [151] detailed study of temperature-dependent uncertainties on reaction rates allowed them to estimate the magnitude of the uncertainty factor at a temperature different from the one used in the experiment. Their study was based on various rate compilations [152,153] providing some Arrhenius coefficients, activation temperatures, and their associated errors at a given temperature. Following DeMore et al. [153], Stewart and Thompson [151] were then able to calculate the propagation of the errors at different temperatures, especially at low temperatures. In their critical review, Baulch et al. [20] emphasize however the difficulty of estimating these uncertainties on reaction rates and support the fact that many of them, if known, might be underestimated. Hence, the importance of the kind of experimental studies providing rates at low temperature, useful as they are to reduce the amount of uncertainty in some reactions.

An estimate of the uncertainty of the reaction rate k_i at any given temperature, $F_i(T)$, may be obtained from the following expression adapted from Sander et al. [18]:

$$F_i(T) = F_i(300\,\mathrm{K})\,e^{g_i((1/T)-(1/300))} \quad (3)$$

where $F_i(300\,\mathrm{K})$ is the uncertainty in the rate constant k_i at $T = 300$ K. $F_i = 1.25$ means a precision of k_i within 25%, $F_i = 1.5$ within 50%, $F_i = 2$ within 100%, etc. The coefficient g_i has been defined in this evaluation for use with $F_i(300\,\mathrm{K})$ in the above expression to obtain the rate constant uncertainty at different temperatures. Both uncertainty factors, $F_i(300\,\mathrm{K})$ and g_i, do not necessarily result from a rigorous statistical analysis of the available data. Rather, they have been evaluated to construct the appropriate uncertainty factor, $F_i(T)$, following an approach based on the fact that rate constants are almost always known with a minimum uncertainty at room temperature, supposedly constant within the temperature range of experiments but not within the temperature range of interest to the study of planetary atmospheres. Recent measurements of the rate constant for the reaction of the methylidine radical (CH) with hydrocarbons at very low temperatures show indeed that the behavior of rate coefficients may be different from that expected by the extrapolation of high temperature experiments to low temperatures [37]. The overall uncertainty then normally increases at lowest temperatures, usually because of this lack of experimen-

[1] http://www.udfa.net.

tal data. In addition, data obtained at temperatures far distant from 300 K may be less accurate than at room temperature due to various experimental difficulties. g_i, called from this point the "uncertainty-extrapolating" coefficient, should therefore not be interpreted as the uncertainty in the Arrhenius activation temperature (E_i/R). Both $F_i(300\,\mathrm{K})$ and g_i additional parameters thus quantify the temperature-dependent uncertainties carried by the standard set of coefficients k_i for bi- and trimolecular reactions in a temperature range adapted for exhaustively describing Titan's atmosphere. The uncertainty represented by $F_i(T)$ is normally symmetric; i.e., the rate constant may be greater or smaller than the recommended value, $k_i(T)$, by the factor $F_i(T)$. No cases of asymmetric uncertainties have been given in this evaluation.

We based this evaluation in a fraction of the reactions rates on previous compilations where their uncertainty factors at room temperature $F_i(300\,\mathrm{K})$ have been previously evaluated with values included between 1.05 and 10 [25,26,23,24]. Some of our choices may seem arbitrary but were motivated by several arguments. For reactions whose uncertainty factors $F_i(300\,\mathrm{K})$ were not available, either not considered by these compilations or not estimated because of a lack of experimental set of data, we assumed $F_i(300\,\mathrm{K}) = 2.0$ and $g_i = 100$. As there is no obvious reason to assume that these reactions are affected, on average, by a larger uncertainty than the others, we therefore chose to assign them the precision that dominates the above compiled reactions set and/or their own review (more than 25% of the reactions have $F_i(300\,\mathrm{K}) = 2.0$ and more than 50% have $g_i = 100$). Besides, a lack of laboratory or theoretical measurements usually enforces modelers to estimate some chemical rate coefficients for several reactions, based on analogies in molecular structures and exothermicities. We assumed for these reactions $F_i(300\,\mathrm{K}) = 10.0$, the highest imprecision that can be found in the compilations, but still associated with $g_i = 100$. By assuming a higher uncertainty on reactions without known $F_i(300\,\mathrm{K})$ factor and/or on estimated reactions, any selection method to identify the key reactions responsible for the greatest imprecision in theoretical models would tend to point inevitably to them, even if their rate coefficients are already known to be considered with priority in order to have their uncertainty better constrained.

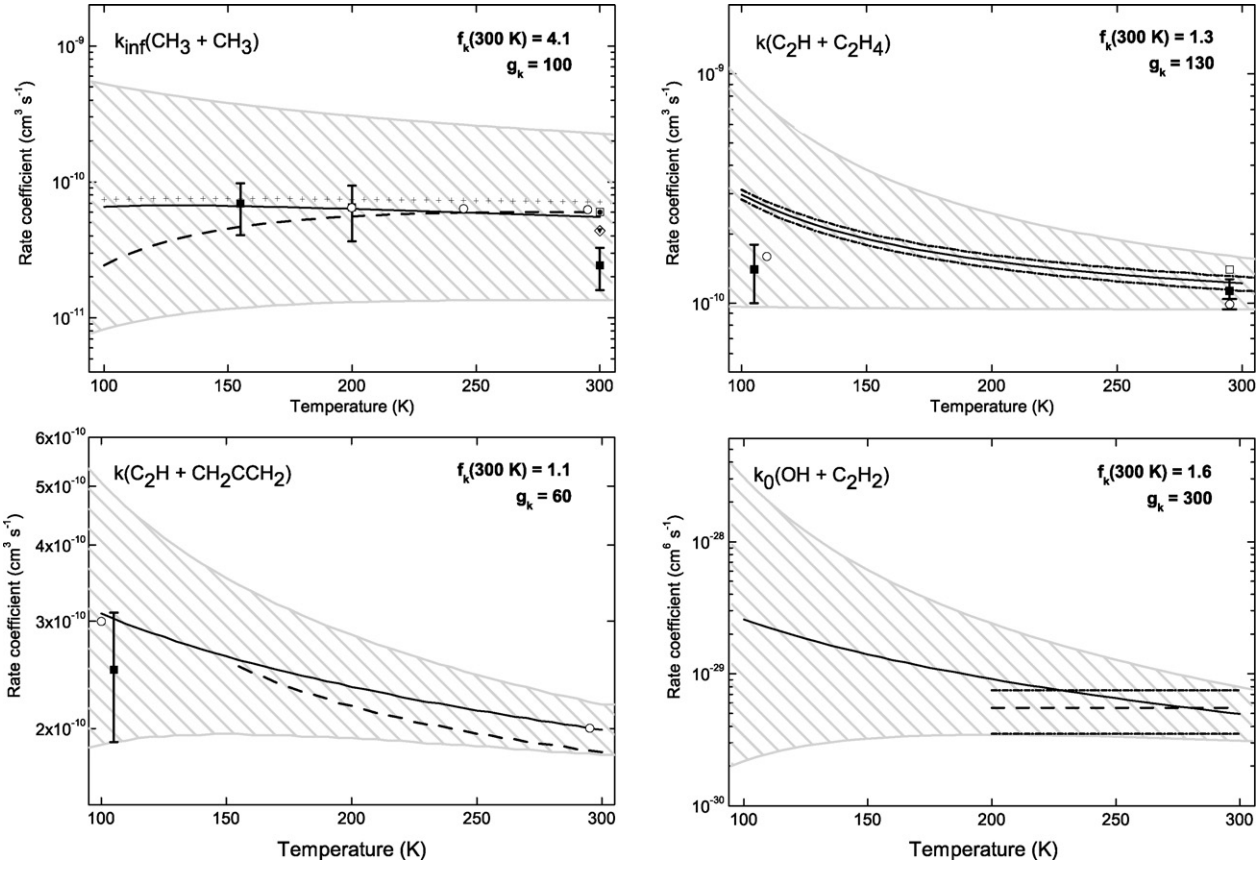

Fig. 3. Examples of rate coefficients and their 1 σ-attached uncertainties, as a function of temperature, as reviewed and implemented in our Monte-Carlo study. (a) $CH_3 + CH_3$ high-pressure, two-body limiting reaction rate—nominal rate coefficient used to generate our nominal 1D profiles taken from Wang et al. [53](solid line), Klippenstein and Harding [52](open circles), Cody et al. [50,51](filled squares), Slagle et al. [45](dashed line), Baulch et al. [26](open squares), Tsang and Hampson [23](open diamond), Tsang [24](filled triangle). (b) $C_2H + C_2H_4$ reaction rate—nominal rate coefficient used to generate our nominal 1D profiles taken from Opansky and Leone [82](solid line with its associated experimental uncertainties), Chastaing et al. [83](open circles), Vakhtin et al. [85](filled squares), Laufer and Fahr [160](open squares). (c) $C_2H + CH_2CCH_2$ reaction rate—nominal rate coefficient used to generate our nominal 1D profiles taken from Carty et al. [84], Laufer and Fahr [160](open circles), Vakhtin et al. [86](filled squares), Hoobler and Leone [80](dashed line). (d) $OH + C_2H_2$ low-pressure, three-body limiting reaction rate—nominal rate coefficient used to generate our nominal 1D profiles taken from Atkinson et al. [161], DeMore et al. [162](dashed line with its associated experimental uncertainties). k_D, the absolute limit rate in pure N_2, is also considered.

Some examples of such adopted uncertainty limits, as a function of temperature, as inferred from our estimations, are shown on (see Fig. 3 a–d). The whole set of adopted nominal reaction rates is displayed along with their uncertainty parameters in Table 2; the adopted uncertainty factors at room temperature $F_i(300\,\mathrm{K})$ range from 1.1 to 12 and their attached "uncertainty-extrapolating" coefficients g_i from 30 to 600.

4. Implications for planetary atmospheres modeling

As we have seen in this review of the main chemical reactions used in the latest models, many uncertainties still remain concerning rate constants, absorption cross sections and quantum yields as well as the role of potential excited states. Our adopted uncertainty factors at room temperature $F_i(300\,\mathrm{K})$ range from 1.1 to 12 and their attached "uncertainty-extrapolating" coefficients g_i from 30 to 600. These assigned uncertainties represent our own subjective assessment but these range seems reasonable when confronted to Earth-based, higher temperature kinetic databases. Extensive experimental studies are necessary to improve our knowledge of photochemical parameters, especially at low temperature. They are important in order to evaluate precisely the uncertainty factors of these rates and to lower these uncertainties at low temperatures and represent an important prerequisite before to allow modelers to specifically pinpoint the photochemical parameters that are responsible for inducing the largest uncertainties in a more representative way (using photochemical models or other techniques such as the one developed by Dobrijevic et al. [154]). It would allow eventually a more efficient use of photochemical modeling in orientating future laboratory investigations and confronting their computed results to the insights provided by the observations.

Very recently, studies have been performed in order to evaluate the effect of imprecisions in photochemical rates on computed concentrations of hydrocarbons obtained with photochemical models of Titan's atmosphere [15,17]. Although restricted to 0D box approximations, these calculations exhibit quite startling results: considering realistic uncertainties regarding photochemical parameters, imprecision in computed hydrocarbon concentrations in the low atmosphere may extend over a few orders of magnitude. Hébrard et al. [17] thus asserted that intrinsic imprecision in photochemical models may be as significant as to question indeed any comparisons between theoretical models with observations and that any potential conclusions subsequently inferred.

The evaluation of uncertainties in photochemical parameters in conditions representative of Titan's atmosphere, following our investigation of their photochemical sources as detailed above, is also a fruitful requirement for improving Hébrard et al. [17] calculations. These improvements concern its extension to a 1D model including transport processes and a detailed study of the effects of radiative transfer calculation on photodissociation rates. Any further work should also be extended to nitrogen and oxygen photochemistry for a better discussion on the mechanisms involved in heavy compounds formation in Titan's atmosphere. Our better determination of uncertainties in photolysis and reaction rates as a function of temperature is an essential tool to study Titan's atmosphere this way. More generally, such an exhaustive database would be essential for all studies related to planetary atmospheres. Unfortunately, to our knowledge, such databases do not exist except now specifically for Titan's atmosphere.

Appendix A

Table 1: Chemical reactions scheme and their associated uncertainties

	Reactions	Rate coefficients	$F(300\ K)$	g	References
R1	$H + H \xrightarrow{M} H_2$	$1.5 \times 10^{-29}\ T^{-1.3}$	1.70	100*	Tsang and Hampson [1986]
R2	$H + CH \longrightarrow C + H_2$	$1.31 \times 10^{-10}\ e^{-80/T}$	10.00	100*	Harding *et al.* [1993]
R3	$H + {}^1CH_2 \longrightarrow CH + H_2$	2.71×10^{-10}	2.00*	100	Tsang and Hampson [1986]
R4	$H + {}^3CH_2 \longrightarrow CH + H_2$	$3.54 \times 10^{-11}\ T^{0.32}$	10.00*	600	Fulle and Hippler [1997]
R5	$H + {}^3CH_2 \xrightarrow{M} CH_3$	$k_0 = 3.1 \times 10^{-30}\ e^{457/T}$	2.00	100	Gladstone [1996]
		$k_\infty = 1.5 \times 10^{-10}$	2.00	100	
R6	$H + CH_3 \longrightarrow {}^3CH_2 + H_2$	$1.0 \times 10^{-10}\ e^{-7600/T}$	10.00*	100	Baulch *et al.* [1992]
R7	$H + CH_3 \xrightarrow{M} CH_4$	$k_0 = 6.33 \times 10^{-21}\ T^{-2.98}\ e^{-635/T}$	2.60	400	Forst *et al.* [1991]
		$k_\infty = 3.5 \times 10^{-10}$	1.40	100*	Baulch *et al.* [1994]
R8	$H + CH_4 \longrightarrow CH_3 + H_2$	$2.18 \times 10^{-20}\ T^3\ e^{-4045/T}$	1.58	100	Baulch *et al.* [1992]
R9	$H + C_2H \xrightarrow{M} C_2H_2$	$k_0 = 1.26 \times 10^{-18}\ T^{-3.1}\ e^{-721/T}$	2.00	100	Tsang and Hampson [1986]
		$k_\infty = 3.0 \times 10^{-10}$	1.50	100	
R10	$H + C_2H_2 \longrightarrow C_2H + H_2$	$1.0 \times 10^{-10}\ e^{-11200/T}$	5.00	100	Tsang and Hampson [1986]
R11	$H + C_2H_2 \xrightarrow{M} C_2H_3$	$k_0 = 3.3 \times 10^{-30}\ e^{-740/T}$	3.16	100*	Baulch *et al.* [1994]
		$k_\infty = 1.4 \times 10^{-11}\ e^{-1300/T}$	8.00	100*	
R12	$H + C_2H_3 \longrightarrow C_2H_2 + H_2$	7.6×10^{-11}	4.00	100*	Monks *et al.* [1995]
R13	$H + C_2H_3 \xrightarrow{M} C_2H_4$	$k_0 = 5.76 \times 10^{-24}\ T^{-1.3}$	2.00	100	Monks *et al.* [1995]
		$k_\infty = 8.0 \times 10^{-11}$	2.00	100	
R14	$H + C_2H_4 \xrightarrow{M} C_2H_5$	$k_0 = 7.69 \times 10^{-30}\ e^{-383/T}$	2.40	150	Baulch *et al.* [1994]
		$k_\infty = 6.6 \times 10^{-15}\ T^{1.28}\ e^{-650/T}$	2.00*	170	
R15	$H + C_2H_5 \longrightarrow CH_3 + CH_3$	1.25×10^{-10}	2.20	100*	Sillesen *et al.* [1993]
R16	$H + C_2H_5 \longrightarrow C_2H_4 + H_2$	3.0×10^{-12}	3.00	100	Tsang and Hampson [1986]
R17	$H + C_2H_5 \xrightarrow{M} C_2H_6$	$k_0 = 5.5 \times 10^{-23}\ T^{-2}\ e^{-1040/T}$	2.00	100	Teng and Jones [1972]
		$k_\infty = 1.66 \times 10^{-10}$	1.20	100*	Sillesen *et al.* [1993]
R18	$H + C_2H_6 \longrightarrow C_2H_5 + H_2$	$2.35 \times 10^{-15}\ T^{1.5}\ e^{-3725/T}$	2.00*	100	Baulch *et al.* [1992]
R19	$H + C_3H_2 \xrightarrow{M} C_3H_3$	$k_0 = 1.7 \times 10^{-26}$	2.00	100	Laufer *et al.* [1983]
		$k_\infty = 1.0 \times 10^{-11}$	2.00	100	Homann and Wellmann [1983]
R20	$H + C_3H_3 \xrightarrow{M} CH_3C_2H$	$k_0 = 1.7 \times 10^{-26}$	2.00	100	Laufer *et al.* [1983]
		$k_\infty = 2.5 \times 10^{-10}$	1.90	100*	Atkinson and Hudgens [1999]
R21	$H + C_3H_3 \xrightarrow{M} CH_2CCH_2$	$k_0 = 1.7 \times 10^{-26}$	2.00	100	Laufer *et al.* [1983]
		$k_\infty = 2.5 \times 10^{-10}$	1.90	100*	Atkinson and Hudgens [1999]
R22	$H + CH_3C_2H \xrightarrow{M} CH_3 + C_2H_2$	$k_0 = 8.0 \times 10^{-24}\ T^{-2}\ e^{-1225/T}$	2.00	100	Wagner and Zellner [1972a]
		$k_\infty = 9.7 \times 10^{-13}\ e^{-1550/T}$	2.00	100	
R23	$H + CH_3C_2H \xrightarrow{M} C_3H_5$	$k_0 = 8.0 \times 10^{-24}\ T^{-2}\ e^{-1225/T}$	2.00	100	Whytock *et al.* [1976]
		$k_\infty = 6.0 \times 10^{-11}\ e^{-1233/T}$	2.00	100	
R24	$H + CH_2CCH_2 \longrightarrow CH_3C_2H + H$	$1.29 \times 10^{-11}\ e^{-1156/T}$	2.00	100	Alexetrov *et al.* [1980]
R25	$H + CH_2CCH_2 \xrightarrow{M} CH_3 + C_2H_2$	$k_0 = 8.0 \times 10^{-24}\ T^{-2}\ e^{-1225/T}$	2.00	100	Wagner and Zellner [1972b]
		$k_\infty = 9.7 \times 10^{-13}\ e^{-1550/T}$	2.00	100	
R26	$H + CH_2CCH_2 \xrightarrow{M} C_3H_5$	$k_0 = 8.0 \times 10^{-24}\ T^{-2}\ e^{-1225/T}$	2.00	100	Whytock *et al.* [1976]
		$k_\infty = 6.6 \times 10^{-12}\ e^{-1360/T}$	2.00	100	
R27	$H + C_3H_5 \longrightarrow C_2H_3 + CH_3$	6.0×10^{-11}	10.00	100	Estimated from R34
R28	$H + C_3H_5 \longrightarrow CH_3C_2H + H_2$	3.3×10^{-10}	3.00	100*	Tsang [1991]
R29	$H + C_3H_5 \longrightarrow CH_2CCH_2 + H_2$	3.0×10^{-11}	3.00	100*	Tsang [1991]
R30	$H + C_3H_5 \xrightarrow{M} C_3H_6$	$k_0 = 1.0 \times 10^{-24}$	2.00	100	Hanning-Lee and Pilling [1992]
		$k_\infty = 2.84 \times 10^{-10}$	1.60	100*	
R31	$H + C_3H_6 \longrightarrow CH_3 + C_2H_4$	$1.2 \times 10^{-11}\ e^{-655/T}$	2.00*	100	Tsang [1991]
R32	$H + C_3H_6 \longrightarrow C_3H_5 + H_2$	$2.87 \times 10^{-19}\ T^{2.5}\ e^{-1254/T}$	2.00*	100	Tsang [1991]
R33	$H + C_3H_6 \xrightarrow{M} C_3H_7$	$k_0 = 1.5 \times 10^{-29}$	2.00	100	Laufer *et al.* [1983]
		$k_\infty = 3.7 \times 10^{-11}\ e^{-1040/T}$	2.00*	100*	
R34	$H + C_3H_7 \longrightarrow C_2H_5 + CH_3$	6.0×10^{-11}	2.00	100	Tsang [1988]
R35	$H + C_3H_7 \longrightarrow C_3H_6 + H_2$	3.0×10^{-12}	2.00*	100	Tsang [1988]
R36	$H + C_3H_7 \xrightarrow{M} C_3H_8$	$k_0 = 5.5 \times 10^{-23}\ T^{-2}\ e^{-1040/T}$	10.00	100	Estimated from R17(k_0)
		$k_\infty = 2.49 \times 10^{-10}$	2.00*	100*	Munk *et al.* [1986]
R37	$H + C_3H_8 \longrightarrow C_3H_7 + H_2$	$2.2 \times 10^{-18}\ T^{2.54}\ e^{-3400/T}$	3.00	100	Tsang [1988]
R38	$H + C_4H \xrightarrow{M} C_4H_2$	$k_0 = 1.26 \times 10^{-18}\ T^{-3.1}\ e^{-721/T}$	10.00	100	Estimated from R9(k_0)
		$k_\infty = 3.0 \times 10^{-10}$	10.00	100	Estimated from R9(k_∞)
R39	$H + C_4H_2 \xrightarrow{M} C_4H_3$	$k_0 = 3.3 \times 10^{-30}\ e^{-740/T}$	10.00	100	Estimated from R11(k_0)
		$k_\infty = 1.39 \times 10^{-10}\ e^{-1184/T}$	2.00	100	Nava *et al.* [1986]
R40	$H + C_4H_3 \longrightarrow C_2H_2 + C_2H_2$	3.3×10^{-12}	2.00	100	Schwanebeck and Warnatz [1975]
R41	$H + C_4H_3 \longrightarrow C_4H_2 + H_2$	1.2×10^{-11}	2.00	100	Schwanebeck and Warnatz [1975]
R42	$H + C_4H_3 \xrightarrow{M} C_4H_4$	$k_0 = 5.76 \times 10^{-24}\ T^{-1.3}$	2.00	100	Estimated from R13(k_0)
		$k_\infty = 8.56 \times 10^{-10}\ e^{-405/T}$	2.00	100	Duran *et al.* [1988]
R43	$H + C_4H_4 \xrightarrow{M} C_4H_5$	$k_0 = 8.76 \times 10^{-08}\ T^{-7.03}\ e^{-1390/T}$	2.00	100	Schwanebeck and Warnatz [1975]
		$k_\infty = 3.3 \times 10^{-12}$	2.00	100	
R44	$H + C_4H_6 \longrightarrow C_4H_5 + H_2$	$1.05 \times 10^{-13}\ T^{0.7}\ e^{-3019/T}$	2.00	100	Weissman and Benson [1988]
R45	$H + C_6H \xrightarrow{M} C_6H_2$	$k_0 = 1.26 \times 10^{-18}\ T^{-3.1}\ e^{-721/T}$	2.00	100	Kiefer and von Drasek [1990]
		$k_\infty = 3.0 \times 10^{-10}$	2.00	100	
R46	$H + C_6H_4 \xrightarrow{M} C_6H_5$	$k_0 = 1.96 \times 10^{+33}\ T^{-18.35}\ e^{-6694/T}$	2.00	100	Wang and Frenklach [1994]
		$k_\infty = 1.06 \times 10^{-14}\ T^{1.11}\ e^{-705/T}$	2.00	100	
R47	$H + C_6H_5 \xrightarrow{M} C_6H_6$	$k_0 = 1.82 \times 10^{+28}\ T^{-16.3}\ e^{-3526/T}$	2.00	100	Wang and Frenklach [1997]
		$k_\infty = 1.66 \times 10^{-10}$	2.00	100	
R48	$H + C_6H_6 \longrightarrow C_6H_5 + H_2$	$4.15 \times 10^{-10}\ e^{-8052/T}$	2.00	100	Wang and Frenklach [1997]
R49	$H + C_6H_6 \xrightarrow{M} C_6H_7$	$k_0 = 3.3 \times 10^{-30}\ e^{-740/T}$	10.00	100	Estimated from R11(k_0)
		$k_\infty = 5.27 \times 10^{-11}\ e^{-1605/T}$	2.00	100	Mebel *et al.* [1997]
R50	$C + H_2 \xrightarrow{M} {}^3CH_2$	$k_0 = 7.0 \times 10^{-32}$	1.30	100*	Husain *et al.* [1975]
		$k_\infty = 2.06 \times 10^{-11}\ e^{-55.4/T}$	2.00	100	Harding *et al.* [1993]
R51	$C + C \xrightarrow{M} C_2$	$k_0 = 4.87 \times 10^{-27}\ T^{-1.6}$	2.00	100	Slack *et al.* [1976]
		$k_\infty = 2.16 \times 10^{-11}$	2.00	100	Martinotti *et al.* [1968]
R53	$C + CH_4 \longrightarrow C_2H_4$	2.0×10^{-15}	3.00	100	Husain *et al.* [1971] - Upper limit
R54	$C + C_2H_2 \longrightarrow C_3H_2$	$4.6 \times 10^{-10}\ T^{-0.08}$	2.00*	50	Chastaing *et al.* [1999]
R55	$C + C_2H_4 \longrightarrow CH_2CCH_2$	$4.6 \times 10^{-10}\ T^{-0.07}$	1.80	50	Chastaing *et al.* [1999]
R56	$C + CH_3C_2H \longrightarrow C_4H_4$	8.0×10^{-10}	2.20	100*	Husain *et al.* [1997]

Table 2: Photodissociations scheme used in the model

Pathways		Cross sections	F_σ	Quantum yields		F_q
J1	$H_2 + h\nu \longrightarrow H + H$	Atreya (1986)				
J2	$CH_3 + h\nu \longrightarrow {}^1CH_2 + H$	Okabe (1978)	1.2	1,0 [216 nm]	Parkes (1973)	
J3a	$CH_4 + h\nu \longrightarrow CH_3 + H$	Chen and Wu (2004) at 150 K [120-142]	1.15	1,0 [>120 nm]; 0.291 [Lyman α]	Wang *et al.* (2000)	1.5
J3b	$\longrightarrow {}^1CH_2 + H + H$	and 370 K [142-143]		0.055 [Lyman α]		
J3c	$\longrightarrow {}^1CH_2 + H_2$			0.584 [Lyman α]		
J3d	$\longrightarrow CH + H_2 + H$			0.07 [Lyman α]		
J4a	$C_2H_2 + h\nu \longrightarrow C_2H + H$	Wu et al. (2001) at 150 K [117-211]	1.35	0.3	Okabe (1981); Okabe (1983);	1.5
J4b	$\longrightarrow C_2 + H_2$	and 295 K [215-225]		0.1	Seki and Okabe (1993)	
J5	$C_2H_3 + h\nu \longrightarrow C_2H_2 + H$	Fahr *et al.* (1998)	1.35	1.0	Fahr *et al.* (1998)	
J6a	$C_2H_4 + h\nu \longrightarrow C_2H_2 + H_2$	Wu et al. (2004) at 140 K	1.2	0.58 [118-174]; 0.73 [175-210]	Holland *et al.* (1997);	1.25
J6b	$\longrightarrow C_2H_2 + H + H$			0.42 [118-174]; 0.27 [175-210]	Chang *et al.* (1998)	
J7a	$C_2H_6 + h\nu \longrightarrow C_2H_4 + H_2$	Chen and Wu (2004) at 150 K	1.2	0.56 [113-170]; 0.12 [Lyman α]	Akimoto *et al.* (1965);	1.25
J7b	$\longrightarrow C_2H_4 + H + H$			0.14 [113-170]; 0.30 [Lyman α]	Hampson and McNesby (1965);	
J7c	$\longrightarrow C_2H_2 + H_2 + H_2$			0.27 [113-170]; 0.25 [Lyman α]	Lias *et al.* (1970);	
J7d	$\longrightarrow CH_4 + {}^1CH_2$			0.02 [113-170]; 0.25 [Lyman α]	Mount and Moos (1978)	
J7e	$\longrightarrow CH_3 + CH_3$			0.01 [113-170]; 0.08 [Lyman α]	Mount and Moos (1978)	
J8a	$C_3H_3 + h\nu \longrightarrow C_3H_2 + H$	Fahr *et al.* (1997)	1.35	0.96 [230-300]	Jackson *et al.* (1991)	1.25
J8b	$\longrightarrow C_3H + H_2$			0.04 [230-300]		
J9a	$CH_3C_2H + h\nu \longrightarrow C_3H_3 + H$	Chen *et al.* (2000) at 200 K	1.4	0.56 [120-220]	Ho *et al.* (1998);	1.1
J9b	$\longrightarrow C_3H_2 + H_2$			0.44 [120-220]	Sun *et al.* (1999)	
J10a	$CH_2CCH_2 + h\nu \longrightarrow C_3H_3 + H$	Chen *et al.* (2000) at 295 K [120-129]	1.4	0.64 [120-233]	Seki and Okabe (1992);	1.1
J10b	$\longrightarrow C_3H_2 + H_2$	and 200 K [130-233]		0.36[120-233]	Ni *et al.* (1999); Sun *et al.* (1999)	
J11a	$C_3H_6 + h\nu \longrightarrow C_3H_5 + H$	Samson (1962) [120-160];	1.45	0 [120-135]; 0 [136-155]; 0.565 [156-175]; 0.41 [176-195]	Collin (1988)	1.25
J11b	$\longrightarrow CH_3C_2H + H_2$	Fahr and Nayak (1996) at 223 K [160-200]		0.11 [120-135]; 0.11 [136-155]; 0.01 [156-175]; 0.01 [176-195]		
J11c	$\longrightarrow CH_2CCH_2 + H_2$			0.17 [120-135]; 0.22 [136-155]; 0.01 [156-175]; 0.01 [176-195]		
J11d	$\longrightarrow C_2H_4 + {}^1CH_2$			0.06 [120-135]; 0.04 [136-155]; 0.02 [156-175]; 0.03 [176-195]		
J11e	$\longrightarrow C_2H_3 + CH_3$			0.21 [120-135]; 0.27 [136-155]; 0.335 [156-175]; 0.4 [176-195]		
J11f	$\longrightarrow C_2H_2 + CH_4$			0.05 [120-135]; 0.03 [136-155]; 0.05 [156-175]; 0.04 [176-195]		
J12a	$C_3H_8 + h\nu \longrightarrow C_3H_6 + H_2$	Calvert and Pitts (1966)	1.35	0.34 [120-135]; 0.66 [136-154]; 0.94 [155-163]	Johnston *et al.* (1978)	1.25
J12b	$\longrightarrow C_2H_6 + {}^1CH_2$			0.09 [120-135]; 0.04 [136-154]; 0 [155-163]		
J12c	$\longrightarrow C_2H_5 + CH_3$			0.35 [120-135]; 0.19 [136-154]; 0 [155-163]		
J12d	$\longrightarrow C_2H_4 + CH_4$			0.22 [120-135]; 0.11 [136-154]; 0.06 [155-163]		
J13a	$C_4H_2 + h\nu \longrightarrow C_4H + H$	Kloster-Jensen *et al.* (1974) [120-160];	1.65	0.2 [120-180]; 0 [181-205]: 0 (206-264]	Glicker and Okabe (1987)	1.5
J13b	$\longrightarrow C_2H_2 + C_2$	Fahr and Nayak (1994) at 223 K [160-196];		0.1 [120-180]; 0.06 [181-205]; 0 [206-264]		

Appendix B. Supplementary data

Supplementary data associated with this article can be found, in the online version, at doi:10.1016/j.jphotochemrev.2006.12.004.

References

[1] F. Raulin, T. Owen, Organic chemistry and exobiology on Titan, Space Sci. Rev. 104 (1/2) (2002) 377–394.

[2] Y. Yung, M. Allen, J. Pinto, Photochemistry of the atmosphere of Titan—comparison between model and observations, Astrophys. J. Suppl. S. 55 (3) (1984) 465–506.

[3] D. Toublanc, J. Parisot, J. Brillet, D. Gautier, F. Raulin, C. McKay, Photochemical modeling of Titan's atmosphere, Icarus 113 (1) (1995) 2–26.

[4] L. Lara, E. Lellouch, J. Lòpez-Moreno, R. Rodrigo, Vertical distribution of Titan's atmospheric neutral constituents, J. Geophys. Res. Planets 101 (E10) (1996) 23261–23284.

[5] J. Dire, Seasonal photochemical and meridional transport model for the stratosphere of Titan, Icarus 145 (2) (2000) 428–444.

[6] S. Lebonnois, D. Toublanc, F. Hourdin, P. Rannou, Seasonal variations of Titan's atmospheric composition, Icarus 152 (2) (2001) 384–406.

[7] E. Wilson, S. Atreya, Current state of modeling the photochemistry of Titan's mutually dependent atmosphere and ionosphere, J. Geophys. Res. Planets 109 (E6) (2004) 06002.

[8] P. Rannou, F. Hourdin, C. McKay, D. Luz, A coupled dynamics–microphysics model of Titan's atmosphere, Icarus 170 (2) (2004) 443–462.

[9] P. Rannou, F. Montmessin, F. Hourdin, S. Lebonnois, On the latitudinal distribution of clouds on Titan, Science 311 (2006) 201–205.

[10] E. Wilson, S. Atreya, Chemical sources of haze formation in Titan's atmosphere, Planet. Space Sci. 51 (14/15) (2003) 1017–1033.

[11] S. Lebonnois, Benzene and aerosol production in Titan and Jupiter's atmospheres: a sensitivity study, Planet. Space Sci. 53 (5) (2005) 486–497.

[12] Y. Sekine, H. Imanaka, B. Khare, E. Bakes, C. McKay, S. Sugita, T. Matsui, An experimental study on interactions between Titan tholin and H atom, Bull. Am. Astron. Soc. 37 (2005) 722.

[13] D. Strobel, Photochemistry in outer solar system atmospheres, Space Sci. Rev. 116 (1/2) (2005) 155–170.

[14] M. Dobrijevic, J. Parisot, Effect of chemical kinetics uncertainties on hydrocarbon production in the stratosphere of Neptune, Planet. Space Sci. 46 (5) (1998) 491–505.

[15] N. Smith, Sensibilité des modèles théoriques de l'atmosphère de Titan aux incertitudes sur la photochimie des hydrocarbures simples, Ph.D. Thesis, Université Paris, Val de Marne (Paris XII), Créteil, 1999.

[16] M. Dobrijevic, J. Ollivier, F. Billebaud, J. Brillet, J. Parisot, Effect of chemical kinetic uncertainties on photochemical modeling results: application to Saturn's atmosphere, Astron. Astrophys. 398 (1) (2003) 335–344.

[17] E. Hébrard, Y. Bénilan, F. Raulin, Sensitivity effects of photochemical parameters uncertainties on hydrocarbon production in the atmosphere of Titan, Adv. Space Res. 36 (2005) 268–273.

[18] S. Sander, R. Friedl, D. Golden, M. Kurylo, R. Huie, V. Orkin, G. Moortgat, A. Ravishankara, C. Kolb, M. Molina, B. Finlayson-Pitts, Chemical kinetics and photochemical data for use in atmospheric studies. Evaluation No. 14, JPL Publication 02-25, 2003, pp. 1–334.

[19] R. Atkinson, D. Baulch, R. Cox, R. Hampson, J. Kerr, M. Rossi, J. Troe, Evaluated kinetic and photochemical data for atmospheric chemistry, organic species: supplement VII, J. Phys. Chem. Ref. Data 28 (2) (1999) 191–393.

[20] D. Baulch, C. Bowman, C. Cobos, R. Cox, T. Just, J. Kerr, M. Pilling, D. Stocker, J. Troe, W. Tsang, R. Walker, J. Warnatz, Evaluated kinetic data for combustion modeling: supplement II, J. Phys. Chem. Ref. Data 34 (3) (2005) 757–1397.

[21] Y. Le Teuff, T. Millar, A. Markwick, The UMIST database for astrochemistry, Astron. Astrophys. Sup. 146 (1) (2000) 157–168.

[22] H. Okabe, Photochemistry of small molecules, John Wiley and Sons, New York, 1978.

[23] W. Tsang, R. Hampson, Chemical kinetic database for combustion chemistry. 1. Methane and related-compounds, J. Phys. Chem. Ref. Data 15 (3) (1986) 1087–1279.

[24] W. Tsang, Chemical kinetic database for combustion chemistry. 3. Propane, J. Phys. Chem. Ref. Data 17 (2) (1988) 887–952.

[25] D. Baulch, C. Cobos, R. Cox, C. Esser, P. Frank, T. Just, J. Kerr, M. Pilling, J. Troe, R. Walker, J. Warnatz, Evaluated kinetic data for combustion modeling, J. Phys. Chem. Ref. Data 21 (3) (1992) 411–734.

[26] D. Baulch, C. Cobos, R. Cox, P. Frank, G. Hayman, T. Just, J. Kerr, T. Murrells, M. Pilling, J. Troe, R. Walker, J. Warnatz, Evaluated kinetic data for combustion modeling: supplement I, J. Phys. Chem. Ref. Data 23 (6) (1994) 847–1033.

[27] J. Moses, B. Bézard, E. Lellouch, G. Gladstone, H. Feuchtgruber, M. Allen, Photochemistry of Saturn's atmosphere. I. Hydrocarbon chemistry and comparisons with ISO observations, Icarus 143 (2) (2000) 244–298.

[28] P. Cook, M. Ashfold, Y. Jee, K. Jung, S. Harich, X. Yang, Vacuum ultraviolet photochemistry of methane, silane and germane, Phys. Chem. Chem. Phys. 3 (10) (2001) 1848–1860.

[29] C. Romanzin, M.-C. Gazeau, Y. Bénilan, E. Hébrard, A. Jolly, F. Raulin, S. Boyé-Péronne, S. Douin, D. Gauyacq, Methane photochemistry: a brief review in the frame of a new experimental program of Titan's atmosphere simulations, Adv. Space Res. 36 (2005) 258–267.

[30] J. Wang, K. Liu, Z. Min, H. Su, R. Bersohn, J. Preses, J. Larese, Vacuum ultraviolet photochemistry of CH_4 and isotopomers. II. Product channel fields and absorption spectra, J. Chem. Phys. 113 (10) (2000) 4146–4152.

[31] G. Mount, H. Moos, Photoabsorption cross-sections of methane and ethane, 1380–1600 Å, at $T = 295$ K and $T = 200$ K, Astrophys. J. 224 (1) (1978) L35–L38.

[32] A. Lee, Y. Yung, B. Cheng, M. Bahou, C. Chung, Y. Lee, Enhancement of deuterated ethane on Jupiter, Astrophys. J. 551 (1) (2001) L93–L96.

[33] F. Chen, C. Wu, Temperature-dependent photoabsorption cross sections in the VUV–UV region. I. Methane and ethane, J. Quant. Spectrosc. Radiat. Transfer 85 (2) (2004) 195–209.

[34] K. Watanabe, M. Zelikoff, E. Inn, 53-23, Tech. Rep., Air Force Cambridge Research Center, 1953.

[35] G. Mount, E. Warden, H. Moos, Photoabsorption cross-sections of methane from 1400 to 1850 Å, Astrophys. J. 214 (1) (1977) L47–L49.

[36] F. Hayes, W. Lawrance, W. Staker, K. King, Temperature dependences of singlet methylene removal rates, J. Phys. Chem. 100 (27) (1996) 11314–11318.

[37] A. Canosa, I. Sims, D. Travers, I. Smith, B. Rowe, Reactions of the methylidine radical with CH_4, C_2H_2, C_2H_4, C_2H_6, and but-1-ene studied between 23 and 295 K with a CRESU apparatus, Astron. Astrophys. 323 (2) (1997) 644–651.

[38] M. Berman, J. Fleming, A. Harvey, M. Lin, Temperature-dependence of the reactions of CH radicals with unsaturated-hydrocarbons, Chem. Phys. 73 (1/2) (1982) 27–33.

[39] M. Berman, M. Lin, Kinetics and mechanisms of the reactions of CH with CH_4, C_2H_6 and n-C_4H_{10}, Chem. Phys. 82 (3) (1983) 435–442.

[40] P. Fleurat-Lessard, J. Rayez, A. Bergeat, J. Loison, Reaction of methylidyne CH($X_2\Pi$) radical with CH_4 and H_2S: overall rate constant and absolute atomic hydrogen production, Chem. Phys. 279 (2/3) (2002) 87–99.

[41] K. McKee, M. Blitz, K. Hughes, M. Pilling, H. Qian, A. Taylor, P. Seakins, H atom branching ratios from the reactions of CH with C_2H_2, C_2H_4, C_2H_6, and neo-C_5H_{12} at room temperature and 25 Torr, J. Phys. Chem. A 107 (30) (2003) 5710–5716.

[42] N. Galland, F. Caralp, Y. Hannachi, A. Bergeat, J. Loison, Experimental and theoretical studies of the methylidyne CH($X^2\Pi$) radical reaction with ethane (C_2H_6): overall rate constant and product channels, J. Phys. Chem. A 107 (28) (2003) 5419–5426.

[43] B. Bézard, H. Feuchtgruber, J. Moses, T. Encrenaz, Detection of methyl radicals (CH_3) on Saturn, Astron. Astrophys. 334 (2) (1998) L41–L44.
[44] B. Bézard, P. Romani, H. Feuchtgruber, T. Encrenaz, Detection of the methyl radical on Neptune, Astrophys. J. 515 (2) (1999) 868–872.
[45] I. Slagle, D. Gutman, J. Davies, M. Pilling, Study of the recombination reaction $CH_3 + CH_3 \rightarrow C_2H_6$. 1. Experiment, J. Phys. Chem. 92 (9) (1988) 2455–2462.
[46] S. Atreya, S. Edgington, T. Encrenaz, H. Feuchtgruber, ISO observations of C_2H_2 on Uranus and CH_3 on Saturn: implications for atmospheric vertical mixing in the Voyager and ISO epochs, and a call for relevant laboratory measurements, in: The Universe as seen by ISO, vol. SP-427, ESA, 1999, pp. 149–152.
[47] A. Lee, Y. Yung, J. Moses, Photochemical modeling of CH_3 abundances in the outer Solar System, J. Geophys. Res. Planets 105 (E8) (2000) 20207–20225.
[48] M. Macpherson, M. Pilling, M. Smith, The pressure and temperature dependence of the rate constant for methyl radical recombination over the temperature range 296–577 K, Chem. Phys. Lett. 94 (4) (1983) 430–433.
[49] D. Walter, H. Grotheer, J. Davies, M. Pilling, A. Wagner, Experimental and theoretical study of the recombination reaction $CH_3 + CH_3 \rightarrow C_2H_6$, Proc. Combust. Inst. 23 (1990) 107–113.
[50] R. Cody, W. Payne, R. Thorn, F. Nesbitt, M. Iannone, D. Tardy, L. Stief, Rate constant for the recombination reaction $CH_3 + CH_3 \rightarrow C_2H_6$ at $T = 298$ and 202 K, J. Phys. Chem. A 106 (25) (2002) 6060–6067.
[51] R. Cody, P. Romani, F. Nesbitt, M. Iannone, D. Tardy, L. Stief, Rate constant for the reaction $CH_3 + CH_3 \rightarrow C_2H_6$ at $T = 155$ K and model calculation of the CH_3 abundance in the atmospheres of Saturn and Neptune, J. Geophys. Res. Planets 108 (E11) (2003) 5119.
[52] S. Klippenstein, L. Harding, A direct transition state theory based study of methyl radical recombination kinetics, J. Phys. Chem. A 103 (47) (1999) 9388–9398.
[53] B. Wang, H. Hou, L. Yoder, J. Muckerman, C. Fockenberg, Experimental and theoretical investigations on the methyl–methyl recombination reaction, J. Phys. Chem. A 107 (51) (2003) 11414–11426.
[54] G. Smith, Rate theory of methyl recombination at the low temperatures and pressures of planetary atmospheres, Chem. Phys. Lett. 376 (3-4) (2003) 381–388.
[55] M. Zelikoff, K. Watanabe, Absorption coefficient of ethylene in the vaccum ultraviolet, J. Opt. Soc. Am. 43 (9) (1953) 756–759.
[56] G. Cooper, T. Olney, C. Brion, Absolute, UV and soft X-ray photoabsorption of ethylene by high-resolution dipole (e, e) spectroscopy, Chem. Phys. 194 (1) (1995) 175–184.
[57] D. Holland, D. Shaw, M. Hayes, L. Shpinkova, E. Rennie, L. Karlsson, P. Baltzer, B. Wannberg, A photoabsorption, photodissociation and photoelectron spectroscopy study of C_2H_4 and C_2D_4, Chem. Phys. 219 (1) (1997) 91–116.
[58] C. Wu, F. Chen, D. Judge, Temperature-dependent photoabsorption cross sections in the VUV–UV region: ethylene, J. Geophys. Res. Planets 109 (E7) (2004), E07S15.
[59] N. Smith, M. Gazeau, A. Khelifi, F. Raulin, A combined experimental and theoretical study of the catalytic dissociation of methane by the photolysis of acetylene at 185 nm, Planet. Space Sci. 47 (1-2) (1999) 3–10.
[60] T. Nakayama, K. Watanabe, Absorption and photoionization coefficients of acetylene, propyne and 1-butyne, J. Chem. Phys. 40 (2) (1964) 558–561.
[61] M. Suto, L. Lee, Quantitative photoexcitation and fluorescence studies of C_2H_2 in vacuum ultraviolet, J. Chem. Phys. 80 (10) (1984) 4824–4831.
[62] K. Seki, H. Okabe, Photochemistry of acetylene at 193.3 nm, J. Phys. Chem. 97 (20) (1993) 5284–5290.
[63] C. Wu, T. Chien, G. Liu, D. Judge, J. Caldwell, Photoabsorption and direct dissociation cross-sections ofC_2H_2 in the 1530–1930 Å region—a temperature-dependent study, J. Chem. Phys. 91 (1) (1989) 272–280.
[64] F. Chen, D. Judge, C. Wu, J. Caldwell, H. White, R. Wagener, High-resolution, low-temperature photoabsorption cross-sections of C_2H_2, PH_3, AsH_3 and GeH_4, with application to Saturn's atmosphere, J. Geophys. Res. Planets 96 (E2) (1991) 17519–17527.
[65] P. Smith, K. Yoshino, W. Parkinson, K. Ito, G. Stark, High-resolution, VUV (147–201 nm) photoabsorption cross-sections for C_2H_2 at 195 K and 295 K, J. Geophys. Res. Planets 96 (E2) (1991) 17529–17533.
[66] Y. Bénilan, N. Smith, A. Jolly, F. Raulin, The long wavelength range temperature variations of the mid-UV acetylene absorption coefficient, Planet. Space Sci. 48 (5) (2000) 463–471.
[67] Y. Bénilan, D. Andrieux, P. Bruston, Mid-UV acetylene cross-sections revisited—sample contamination risk in source data, Geophys. Res. Lett. 22 (8) (1995) 897–900.
[68] C. Wu, F. Chen, D. Judge, Measurements of temperature-dependent absorption cross sections of C_2H_2 in the VUV–UV region, J. Geophys. Res. Planets 106 (E4) (2001) 7629–7636.
[69] S. Satyapal, R. Bersohn, Photodissociation of acetylene at 193.3 nm, J. Phys. Chem. 95 (21) (1991) 8004–8006.
[70] K. Shin, J. Michael, Rate constants (296–1700 K) for the reactions $C_2H + C_2H_2 \rightarrow C_4H_2 + H$ and $C_2D + C_2D_2 \rightarrow C_4D_2 + D$, J. Phys. Chem. 95 (15) (1991) 5864–5869.
[71] H. Okabe, Photochemistry of acetylene at 1849 Å, J. Chem. Phys. 78 (3) (1983) 1312–1317.
[72] H. Okabe, Photochemistry of acetylene at 1470 Å, J. Chem. Phys. 75 (6) (1981) 2772–2778.
[73] L. Stief, V. de Carlo, R. Mataloni, Vacuum-ultraviolet photolysis of acetylene, J. Chem. Phys. 42 (9) (1965) 3113–3121.
[74] M. Irion, K. Kompa, UV laser photochemistry of acetylene at 193 nm, Appl. Phys. B: Photo. 27 (4) (1982) 183–186.
[75] A. Laufer, Vinylidene, ($^3B_2$)—an active intermediate in the photolysis of ethylene, J. Photochem. 27 (3) (1984) 267–271.
[76] N. Hashimoto, N. Yonekura, T. Suzuki, Pump-probe measurements of the predissociation reaction time of C_2H_2 from A(^1A_u) state, Chem. Phys. Lett. 264 (5) (1997) 545–550.
[77] D. Mordaunt, M. Ashfold, R. Dixon, P. Loffler, L. Schnieder, K. Welge, Near threshold photodissociation of acetylene, J. Chem. Phys. 108 (2) (1998) 519–526.
[78] A. Lauter, K. Lee, K. Jung, R. Vatsa, J. Mittal, H. Volpp, Absolute primary H atom quantum yield measurements in the 193.3 and 121.6 nm photodissociation of acetylene, Chem. Phys. Lett. 358 (3/4) (2002) 314–319.
[79] R. Hoobler, S. Leone, Rate coefficients for reactions of ethynyl radical (C_2H) with HCN and CH_3CN: implications for the formation of complex nitriles on Titan, J. Geophys. Res. Planets 102 (E12) (1997) 28717–28723.
[80] R. Hoobler, S. Leone, Low-temperature rate coefficients for reactions of the ethynyl radical (C_2H) with C_3H_4 isomers methylacetylene and allene, J. Phys. Chem. A 103 (10) (1999) 1342–1346.
[81] B. Opansky, S. Leone, Low-temperature rate coefficients of C_2H with CH_4 and CD_4 from 154 to 359 K, J. Phys. Chem. 100 (12) (1996) 4888–4892.
[82] B. Opansky, S. Leone, Rate coefficients of C_2H with C_2H_4, C_2H_6, and H_2 from 150 to 359 K, J. Phys. Chem. 100 (51) (1996) 19904–19910.
[83] D. Chastaing, P. James, I. Sims, I. Smith, Neutral-neutral reactions at the temperatures of interstellar clouds—Rate coefficients for reactions of C_2H radicals with O_2, C_2H_2, C_2H_4 and C_3H_6 down to 15 K, Faraday Discuss. 109 (1998) 165–181.
[84] D. Carty, V. Le Page, I. Sims, I. Smith, Low temperature rate coefficients for the reactions of CN and C_2H radicals with allene (CH_2= C= CH_2) and methyl acetylene (CH_3C_2H), Chem. Phys. Lett. 344 (3-4) (2001) 310–316.
[85] A. Vakhtin, D. Heard, I. Smith, S. Leone, Kinetics of reactions of C_2H radical with acetylene, O_2, methylacetylene, and allene in a pulsed Laval nozzle apparatus at $T = 103$ K, Chem. Phys. Lett. 344 (3-4) (2001) 317–324.
[86] A. Vakhtin, D. Heard, I. Smith, S. Leone, Kinetics of C_2H radical reactions with ethene, propene and 1-butene measured in a pulsed Laval nozzle apparatus at $T = 103$ and 296 K, Chem. Phys. Lett. 348 (1/2) (2001) 21–26.
[87] J. Murphy, A. Vakhtin, S. Leone, Laboratory kinetics of C_2H radical reactions with ethane, propane, and *n*-butane at $T = 96$–296 K: implications for Titan, Icarus 163 (1) (2003) 175–181.
[88] B. Ceursters, H. Nguyen, M. Nguyen, J. Peeters, L. Vereecken, The reaction of C_2H radicals with C_2H_6: absolute rate coefficient measurements for $T = 295$–800 K, and quantum chemical study of the

molecular mechanism, Phys. Chem. Chem. Phys. 3 (15) (2001) 3070–3074.
[89] M. Allen, Y. Yung, J. Pinto, Titan—aerosol photochemistry and variations related to the sunspot cycle, Astrophys. J. 242 (1980) L125–L128.
[90] E. de Vanssay, M. Gazeau, J. Guillemin, F. Raulin, Experimental simulation of Titan's organic chemistry at low-temperature, Planet. Space Sci. 43 (1/2) (1995) 25–31.
[91] J. Kiefer, W. Vondrasek, The mechanism of the homogeneous pyrolysis of acetylene, Int. J. Chem. Kinet. 22 (7) (1990) 747–786.
[92] A. Krestinin, Detailed modeling of soot formation in hydrocarbon pyrolysis, Combust. Flame 121 (3) (2000) 513–524.
[93] E. Kloster-Jensen, H. Haink, H. christen, The electronic spectra of unsubstituted mono- to penta-acetylene in the gas phase and in solution in the range 1100 to 4000 AA, Helv. Chim. Acta 57 (6) (1974) 1731–1744.
[94] A. Fahr, A. Nayak, Temperature-dependent ultraviolet-absorption cross-sections of 1,3-butadiene and butadiyne, Chem. Phys. 189 (3) (1994) 725–731.
[95] S. Glicker, H. Okabe, Photochemistry of diacetylene, J. Phys. Chem. 91 (2) (1987) 437–440.
[96] T. Zwier, M. Allen, Metastable diacetylene reactions as routes to large hydrocarbons in Titan's atmosphere, Icarus 123 (2) (1996) 578–583.
[97] J. Lisy, W. Klemperer, Electric deflection studies of metastable acetylene, J. Chem. Phys. 72 (7) (1980) 3880–3883.
[98] V. Vuitton, C. Gee, F. Raulin, Y. Bénilan, C. Crépin, M. Gazeau, Intrinsic lifetime of metastable excited C_4H_2: Implications for the photochemistry of C_4H_2 in Titan's atmosphere, Planet. Space Sci. 51 (13) (2003) 847–852.
[99] H. Cottin, M. Gazeau, Y. Benilan, F. Raulin, Polyoxymethylene as parent molecule for the formaldehyde extended source in comet Halley, Astrophys. J. 556 (1) (2001) 417–420.
[100] A. Fahr, A. Nayak, Kinetics and products of propargyl (C_3H_3) radical self-reactions and propargyl–methyl cross-combination reactions, Int. J. Chem. Kinet. 32 (2) (1999) 118–124.
[101] U. Alkemade, K. Homann, Formation of C_6H_6 isomers by recombination of propynyl in the system sodium vapor propynylhalide, Z. Phy. Chem. Neue Fol. 161 (1989) 19–34.
[102] C. Morter, S. Farhat, J. Adamson, G. Glass, R. Curl, Rate-constant measurement of the recombination reaction $C_3H_3 + C_3H_3$, J. Phys. Chem. 98 (28) (1994) 7029–7035.
[103] L. Lara, E. Lellouch, V. Shematovich, Titan's atmospheric haze: the case for HCN incorporation, Astron. Astrophys. 341 (1) (1999) 312–317.
[104] E. Zipf, M. Gorman, Electron-impact excitation of the singlet states of N_2. 1. The Birge-Hopfield system ($B^1\Pi u$-$X^1\Sigma g+$), J. Chem. Phys. 73 (2) (1980) 813–819.
[105] Y. Itikawa, M. Hayashi, A. Ichimura, K. Onda, K. Sakimoto, K. Takayanagi, M. Nakamura, H. Nishimura, T. Takayanagi, Cross-sections for collisions of electrons and photons with nitrogen molecules, J. Phys. Chem. Ref. Data 15 (3) (1986) 985–1010.
[106] L. Capone, J. Dubach, S. Prasad, R. Whitten, Galactic cosmic-rays and N_2 dissociation on Titan, Icarus 55 (1) (1983) 73–82.
[107] C. Sagan, W. Thompson, Production and condensation of organic gases in the atmosphere of Titan, Icarus 59 (2) (1984) 133–161.
[108] J. Herron, Evaluated chemical kinetics data for reactions of $N(^2D)$, $N(^2P)$, and $N_2(A^3\sigma u+)$ in the gas phase, J. Phys. Chem. Ref. Data 28 (5) (1999) 1453–1483.
[109] B. Fell, I.V. Rivas, D.L. McFadden, Kinetic study of electronically metastable nitrogen atoms, $N(^2D_J)$, by electron spin resonance absorption, J. Phys. Chem. 85 (3) (1981) 224–228.
[110] H. Umemoto, N. Hachiya, E. Matsunaga, A. Suda, M. Kawasaki, Rate constants for the deactivation of $N(2\,^2D)$ by simple hydride and deuteride molecules, Chem. Phys. Lett. 296 (1–2) (1998) 203–207.
[111] T. Takayanagi, Y. Kurosaki, K. Sato, K. Misawa, Y. Kobayashi, S. Tsunashima, Kinetic studies on the $N(^2D, ^2P)$ + CH_4 and CD_4 reactions: the role of nonadiabatic transitions on thermal rate constants, J. Phys. Chem. A 103 (2) (1999) 250–255.
[112] H. Umemoto, T. Nakae, H. Hashimoto, K. Kongo, M. Kawasaki, Reactions of $N(2\,^2D)$ with methane and deuterated methanes, J. Chem. Phys. 109 (14) (1998) 5844–5848.
[113] H. Umemoto, Y. Kimura, T. Asai, Production of $NH(X^{3\Sigma-})$ radicals in the reaction of $N(^2D)$ with CH_4: nascent and vibrational distributions of NH, Chem. Phys. Lett. 264 (1–2) (1997) 215–219.
[114] Y. Kurosaki, T. Takayanagi, K. Sato, T. S., Ab initio molecular orbital calculations of the potential energy surfaces for the $N(^2D) + CH_4$ reaction, J. Phys. Chem. A 102 (1) (1998) 254–259.
[115] K. Sato, K. Misawa, Y. Kobayashi, M. Matsui, S. Tsunashima, K. Kurosaki, T. Takayanagi, Measurements of thermal rate constants for the reactions of $N(^2D, ^2P)$ with C_2H_4 and C_2D_4 between 225 and 292 K, J. Phys. Chem. A 103 (43) (1999) 8650–8656.
[116] E. Lellouch, P. Romani, J. Rosenqvist, The vertical distribution and origin of HCN in neptune atmosphere, Icarus 108 (1) (1994) 112–136.
[117] G. Black, T. Slanger, G. Stjohn, R. Young, Vacuum-ultraviolet photolysis of N_2O. 4. Deactivation of $N(^2D)$, J. Chem. Phys. 51 (1) (1969) 116–121.
[118] N. Balucani, L. Cartechini, M. Alagia, P. Casavecchia, G. Volpi, Observation of nitrogen-bearing organic molecules from reactions of nitrogen atoms with hydrocarbons: a crossed beam study of $N(^2D)$ + ethylene, J. Phys. Chem. A 104 (24) (2000) 5655–5659.
[119] A. Jolly, Y. Bénilan, T. Ferradaz, N. Fray, M. Schwell, VUV absorption spectroscopy of planetary molecules at low temperature, Bull. Am. Astron. Soc. 37 (2005) 773.
[120] B. Bézard, A. Marten, G. Paubert, Detection of acetonitrile on Titan, B. Am. Astron. Soc. 25 (1993) 1100.
[121] W. Hess, J. Durant, F. Tully, Kinetic-study of the reactions of CN with ethane and propane, J. Phys. Chem. 93 (17) (1989) 6402–6407.
[122] D. Yang, T. Yu, N. Wang, M. Lin, Temperature-dependence of cyanogen radical reactions with selected alkanes—CN reactivities towards primary, secondary and tertiary C—H bonds, Chem. Phys. 160 (2) (1992) 307–315.
[123] I. Sims, J. Queffelec, D. Travers, B. Rowe, L. Herbert, J. Karthauser, I. Smith, Rate constants for the reactions of CN with hydrocarbons at low and ultra-low temperatures, Chem. Phys. Lett. 211 (4/5) (1993) 461–468.
[124] R. Balla, K. Casleton, Kinetic study of the reactions of CN with O_2 and CO_2 from 292 K to 1500 K using high-temperature photochemistry, J. Phys. Chem. 95 (6) (1991) 2344–2351.
[125] L. Copeland, F. Mohammad, M. Zahedi, D. Volman, W. Jackson, Rate constants for CN reactions with hydrocarbons and the product HCN vibrational populations—examples of heavy–light–heavy abstraction reactions, J. Chem. Phys. 96 (8) (1992) 5817–5826.
[126] E. Arunan, G. Manke, D. Setser, Infrared chemiluminescence studies of H + BrCN and H abstraction by CN reactions—importance of the HNC channel, Chem. Phys. Lett. 207 (1) (1993) 81–87.
[127] J. Ferris, J. Guillemin, Photochemical cycloaddition reactions of cyanoacetylene and dicyanoacetylene, J. Org. Chem. 55 (21) (1990) 5601–5606.
[128] T. Hidayat, A. Marten, B. Bézard, D. Gautier, T. Owen, H. Matthews, G. Paubert, Millimeter and submillimeter heterodyne observations of Titan: the vertical profile of carbon monoxide in its stratosphere, Icarus 133 (1) (1998) 109–133.
[129] M. Gurwell, D. Muhleman, CO on Titan: More evidence for a well-mixed vertical profile, Icarus 145 (2) (2000) 653–656.
[130] E. Lellouch, A. Coustenis, B. Sebag, J. Cuby, M. Lopez-Valverde, B. Schmitt, T. Fouchet, J. Crovisier, Titan's 5 mm window: observations with the very large telescope, Icarus 162 (1) (2003) 125–142.
[131] A. Coustenis, B. Bézard, Titan's atmosphere from Voyager infrared observations. 4. Latitudinal variations of temperature and composition, Icarus 115 (1) (1995) 126–140.
[132] A. Coustenis, A. Salama, E. Lellouch, T. Encrenaz, G. Bjoraker, R. Samuelson, T. de Graauw, H. Feuchtgruber, M. Kessler, Evidence for water vapor in Titan's atmosphere from ISO/SWS data, Astron. Astrophys. 336 (3) (1998) L85–L89.
[133] F. Flasar, 44 co-authors, Titan's atmospheric temperatures, winds, and composition, Science 308 (5724) (2005) 975–978.
[134] H. Feuchtgruber, E. Lellouch, T. de Graauw, B. Bézard, T. Encrenaz, M. Griffin, External supply of oxygen to the giant planets, Nature 389 (1997) 159–162.
[135] R. Samuelson, W. Maguire, R. Hanel, V. Kunde, D. Jennings, Y. Yung, A. Aikin, CO_2 on Titan, J. Geophys. Res. Space 88 (NA11) (1983) 8709–8715.

[136] R. de Avillez Pereira, D. Baulch, M. Pilling, S. Robertson, G. Zeng, Temperature and pressure dependence of the multichannel rate coefficients for the $CH_3 + OH$ system, J. Phys. Chem. A 101 (50) (1997) 9681–9693.

[137] K. Fagerström, A. Lund, G. Mahmoud, J. Jodkowski, E. Ratajczak, Kinetics of the cross reaction between methyl and hydroxyl radicals, Chem. Phys. Lett. 204 (3/4) (1993) 226–234.

[138] C. Fenimore, Destruction of methane in water gas by reaction of CH_3 with OH radicals, Proc. Combust. Inst. 12 (1968) 463–467.

[139] A.-S. Wong, C. Morgan, Y. Yung, T. Owen, Evolution of CO on Titan, Icarus 155 (2) (2002) 382–392.

[140] B. Aumont, S. Szopa, S. Madronich, Modelling the evolution of organic carbon during its gas-phase tropospheric oxidation: development of an explicit model based on a self generating approach, Atmos. Chem. Phys. 5 (2005) 2497–2517.

[141] V. Vuitton, J. Doussin, Y. Bénilan, F. Raulin, M. Gazeau, Experimental and theoretical study of hydrocarbon photochemistry applied to Titan stratosphere, Icarus 185 (1) (2006) 287–300.

[142] F. Chen, D. Judge, C. Wu, Temperature dependent photoabsorption cross sections of allene and methylacetylene in the VUV–UV, region, Chem. Phys. 260 (1/2) (2000) 215–223.

[143] N. Smith, Y. Bénilan, P. Bruston, The temperature dependent absorption cross sections of C_4H_2 at mid ultraviolet wavelengths, Planet. Space Sci. 46 (9/10) (1998) 1215–1220.

[144] A. Fahr, A. Nayak, Temperature dependent ultraviolet absorption cross sections of propylene, methylacetylene and vinylacetylene, Chem. Phys. 203 (3) (1996) 351–358.

[145] A. Fahr, P. Hassanzadeh, D. Atkinson, Ultraviolet absorption spectrum and cross-sections of vinyl (C_2H_3) radical in the 225–238 nm region, Chem. Phys. 236 (1–3) (1998) 43–51.

[146] F. Chen, D. Judge, C. Wu, J. Caldwell, Low and room temperature photoabsorption cross sections of NH_3 in the UV region, Planet. Space Sci. 47 (1/2) (1999) 261–266.

[147] J. Troe, Theory of thermal unimolecular reactions at low-pressures. 1. Solutions of the master equation, J. Chem. Phys. 66 (11) (1977) 4745–4757.

[148] W. DeMore, S. Sander, D. Golden, R. Hampson, M. Kurylo, C. Howard, A. Ravishankara, C. Kolb, M. Molina, Chemical kinetics and photochemical data for use in stratospheric modeling. Evaluation No. 10, JPL Publication 92-20, 1992, pp. 1–239.

[149] G. Gladstone, M. Allen, Y. Yung, Hydrocarbon photochemistry in the upper atmosphere of Jupiter, Icarus 119 (1) (1996) 1–52.

[150] A. Laufer, E. Gardner, T. Kwok, Y. Yung, Computations and estimates of rate coefficients for hydrocarbon reactions of interest to the atmospheres of the outer Solar System, Icarus 56 (3) (1983) 560–567.

[151] R. Stewart, A. Thompson, Kinetic data imprecisions in photochemical rate calculations: Means, medians, and temperature dependence, J. Geophys. Res. - Atmos. 101 (D15) (1996) 20953–20964.

[152] R. Atkinson, D. Baulch, R. Cox, R. Hampson, J. Kerr, J. Troe, Evaluated kinetic and photochemical data for atmospheric chemistry: supplement IV—IUPAC subcommittee on gas kinetic data evaluation for atmospheric chemistry, J. Phys. Chem. Ref. Data 21 (6) (1992) 1125–1568.

[153] W. DeMore, S. Sander, D. Golden, R. Hampson, M. Kurylo, C. Howard, A. Ravishankara, C. Kolb, M. Molina, Chemical kinetics and photochemical data for use in stratospheric modeling. Evaluation No. 11, JPL Publication 94-26, 1994, pp. 1–273.

[154] M. Dobrijevic, J. Parisot, I. Dutour, A study of chemical systems using signal flow graph theory—application to Neptune, Planet. Space Sci. 43 (1/2) (1995) 15–24.

[155] D. Mordaunt, I. Lambert, G. Morley, M. Ashfold, R. Dixon, C. Western, L. Schnieder, K. Welge, Primary product channels in the photodissociation of methane at 121.6 nm, J. Chem. Phys. 98 (3) (1993) 2054–2065.

[156] A. Heck, R. Zare, D. Chandler, Photofragment imaging of methane, J. Chem. Phys. 104 (11) (1996) 4019–4030.

[157] R. Brownsword, M. Hillenkamp, T. Laurent, R. Vatsa, H.-R. Volpp, J. Wolfrum, Quantum yield for H atom formation in the methane dissociation after photoexcitation at the Lyman- α (121.6 nm) wavelength, Chem. Phys. Lett. 266 (1997) 259–266.

[158] P. Romani, Recent rate constant and product measurements of the reactions $C_2H_3 + H_2$ and $C_2H_3 + H$—importance for photochemical modeling of hydrocarbons on Jupiter, Icarus 122 (2) (1996) 233–241.

[159] N. Smith, F. Raulin, Modeling of methane photolysis in the reducing atmospheres of the outer solar system, J. Geophys. Res. Planets 104 (E1) (1999) 1873–1876.

[160] A. Laufer, A. Fahr, Reactions and kinetics of unsaturated C_2 hydrocarbon radicals, Chem. Rev. 104 (6) (2004) 2813–2832.

[161] R. Atkinson, D. Baulch, R. Cox, R. Hampson, J. Kerr, M. Rossi, J. Troe, Evaluated kinetic, photochemical and heterogeneous data for atmospheric chemistry: supplement V—IUPAC subcommittee on gas kinetic data evaluation for atmospheric chemistry, J. Phys. Chem. Ref. Data 26 (1997) 521–1011.

[162] W. DeMore, S. Sander, D. Golden, R. Hampson, M. Kurylo, C. Howard, A. Ravishankara, C. Kolb, M. Molina, Chemical kinetics and photochemical data for use in stratospheric modeling. Evaluation No. 12, JPL Publication 97-4, 1997, pp. 1–266.